의학박사 학위논문

HER2 양성 유방암에서 수술 전 TCHP 치료 반응과 면역 레퍼토리의 의의 분석

Immune repertoire and responses to neoadjuvant TCHP therapy in HER2 positive breast cancer

울산대학교 대학원

의학과

신 준 영

Immune repertoire and response to neoadjuvant TCHP therapy in HER2 positive breast cancer

지도교수 이 희 진

이 논문을 의학박사 학위 논문으로 제출함

2022년 07월

울산대학교 대학원

의학과

신 준 영

신준영의 의학박사 학위 논문을 인준함

심사위원 공 경 엽 (인)

심사위원 이 희 진 (인)

심사위원 김 성 배 (인)

심사위원 이 새 별 (인)

심사위원 박 인 아 (인)

울 산 대 학 교 대 학 원

2022 년 08 월

ABSTRACT

Background: Despite of the great progression in the neoadjuvant treatment of HER2 positive breast cancer with the introduction of trastuzumab, approximately 30-40% of HER2 positive early-stage breast cancer still does not reach pathologic complete response (pCR) (1). Immune repertoires have been reported to have a significant impact on a wide range of diseases, including malignancy. We investigated T cell receptor (TCR) and B cell receptor (BCR) repertoires to find factors predicting the treatment response of HER2 positive early-stage breast cancer.

Materials and methods: Totally, 35 cases of HER2 positive breast cancer treated with neoadjuvant trastuzumab, docetaxel, carboplatin, and pertuzumab (TCHP) were recruited. The entire cases were divided into two experiments, consisting of 10 cases of preliminary experiment and 25 cases of main experiment. In preliminary experiment, the biopsy tissues before TCHP treatment and the surgical tissues after TCHP treatment were compared. In main experiment, the biopsy tissues before TCHP treatment were compared according to TCHP treatment response. T cell repertoire for TRA, TRB, TRG, and TRD, and B cell repertoire for IGH, IGK, and IGL was evaluated. Whole transcriptome sequencing was also done.

Results: In the preliminary experiment, regardless of TCHP response, density and richness of TCR and BCR tended to decrease after the TCHP treatment. SDI was decreased in TCR and increased in BCR. In the main experiment, SDI, density, and length of CDR3 of TCR and BCR repertoires showed no significant difference between pCR and non-pCR groups. Density, richness, frequency of MAIT, public TCR from healthy patients, and p53 targeting sequences also showed no significant difference. HER2 targeting TCR sequences were present only in a few cases of pCR group. When pCR and non-pCR groups subdivided according to the level of tumor infiltrating lymphocytes (TILs), density, richness, and SDI showed no significant difference in pCR/highTIL vs. non-pCR/highTIL and pCR/lowTIL vs. non-pCR/lowTIL. In pCR/lowTIL group showed higher proportion of low frequency clones in TRA (non-pCR/lowTIL, 0.01~0.1%, 63%, <0.01%, 32.9% vs.

pCR/lowTIL, 0.01~0.1%, 45.3%, <0.01%, 51.8%, $p < 0.001$) and TRB (non-pCR/lowTIL, 0.01~0.1%, 26.5%, <0.01%, 72.0% vs. pCR/lowTIL, 0.01~0.1%, 14.7%, <0.01%, 84.1%, $p < 0.001$). The frequency of non-productive TRA and TRB, which has CDR3 sequences with a stop codon or out of frame for amino acids, was significantly higher in non-pCR/lowTIL than pCR/lowTIL group (TRA, 10.6% in non-pCR/lowTIL, 9.5% in pCR/lowTIL, $p = 0.051$; TRB, 6.1% in non-pCR/lowTIL and 4.7% in pCR/lowTIL, $p = 0.002$). When predicting treatment response with frequency of non-productive TCR in lowTIL group, area under curve was 0.833 and 0.976 in TRA and TRB, respectively. The pathways associated with response to steroid hormone, ERK1/ERK2 cascade regulation, and negative regulation of cell growth were up-regulated in the non-pCR group.

Conclusions: The role of diversity, richness, and density of TCR and BCR repertoire as predictive markers for TCHP treatment response was not confirmed. Composition of low frequency clones and frequency of non-productive TCR can be candidates for predictive factor of TCHP treatment response, however, validation study and further research for the physiologic mechanism of non-productive TCR are necessary.

TABLE OF CONTENTS

LIST OF TABLES

LIST OF FIGURES

LIST OF ABBREVIATIONS

HER2	Human epithelial growth factor receptor-2
pCR	Pathologic complete response
TCHP	Trastuzumab, Docetaxel, carboplatin, pertuzumab
TILs	Tumor infiltrating lymphocytes
NGS	Next generation sequencing
TCR	T cell receptor
BCR	B cell receptor
IHC	Immunohistochemistry
FFPE	Formalin-fixed paraffin-embedded
SISH	Silver in situ hybridization
DNP	dinitrophenol
RCB	Residual cancer burden
bp	Base pair
MAIT	Mucosa-associated invariant T cells
CIBERSORT	Cell-type identification by estimating relative subset of RNA transcripts
PAM50	Prediction analysis of microarray 50
SDI	Shannon diversity index
PCA	Principal component analysis
FDR	False discovery rate

1. Introduction

Human epithelial growth factor receptor-2 (HER2) over-expression occurs in 15% to 30% of invasive breast cancer, which is more aggressive and has decreased overall survival (1, 2). The 2015 European Society for Medical Oncology Clinical Practice Guideline (3) and the 2017 US National Comprehensive Cancer Network Guideline on Breast cancer (4) recommended the chemotherapy with trastuzumab (Herceptin©, monoclonal antibody binding to extracellular domain IV of HER2) for the management of HER2 positive early-stage breast cancer in adjuvant therapy. Trastuzumab also improved pathologic complete response (pCR) rate and 10-year overall survival when administrated as combination treatment in early-stage, locally advanced HER2 positive breast cancer (3). Recently, combination of trastuzumab, docetaxel, carboplatin, and pertuzumab (TCHP) has become a favored neoadjuvant regimen in a number of practices (1). However, despite of TCHP neoadjuvant therapy, about 30-40% of HER2 positive breast cancer will remain as a residual tumor (1). Many research endeavors to find out the predictors of treatment response.

The level of tumor infiltrating lymphocytes (TILs) is a well-known positive prognostic and predictive biomarker of triple negative breast cancer (5). Some studies have reported large amount of TILs were associated with pCR rate and disease free survival of HER2 positive breast cancer (6), however, others have reported no relationship (1).

Recently, with the development of high-throughput next generation sequencing (NGS), studies on immune repertoire of T cell receptor (TCR) and B cell receptor (BCR) have been actively conducted, and in some disease groups, immune repertoire has been reported to have a significant influence on the prognosis of disease and pathophysiology (7-9). In this study, we tried to analyze the immune repertoire of TCR and BCR using high-throughput NGS in HER2 positive tumors treated with neoadjuvant TCHP to find out the effect of immune repertoire on TCHP treatment response. In addition, other factors that can help predict treatment responses were analyzed.

2. Materials and methods

2.1. Study materials

2.1.1 Ethical approval

This study was approved from Institutional Review Board of Asan Medical Center (approval number, 2019-0527). Informed consent was obtained from all subjects enrolled.

2.1.2 Study participants

A total of 35 patients with HER2 over-expressed breast cancer were recruited from the Asan Medical Center, Seoul, Republic of Korea. All patients underwent a core-needle biopsy prior to initiating neoadjuvant chemotherapy of TCHP from 2017 to 2020. HER2 over-expression was determined in a core-needle biopsy according to HER2 testing guidelines from the American Society of Clinical Oncology of American Pathologists (10). After neoadjuvant treatment, all patients underwent surgical treatment and disease response (pCR or non-pCR) was pathologically evaluated on the surgical specimens.

Among the 35 patients, 6 cases with high level of TILs (highTIL, ≥10%) with pCR and 4 cases with low level of TILs (lowTIL, <10%) without pCR (non-pCR) were selected and assigned as preliminary experiment. The remaining 25 patients were consecutively collected and allocated for main experiment, consisting of 13 patients with pCR and 12 patients with non-pCR **(Figure 1**).

The preliminary experiment was used to estimate the effect of TCHP on TCR and BCR repertoires by comparing the pre-treatment core-needle biopsy with the surgical samples. In addition, TCR and BCR sequences present in both biopsy specimens before treatment and surgical specimens after TCHP treatment were searched. The main experiment was examined the core-needle biopsy only before the TCHP treatment, comparing the immune repertoire between the groups with pCR and residual tumor in subsequent TCHP treatment response. In addition, to minimize

the effect of TILs on treatment response, highTIL and lowTIL was subdivided, and separately compared for immune repertoire. The highTIL group included 10 cases, composed 7 cases of pCR (pCR/highTIL) and 3 cases of non-pCR group (non-pCR/highTIL). The other 13 cases were defined as lowTIL group, which had 6 cases of pCR (pCR/lowTIL) and 7 case of non-pCR group (non-pCR/lowTIL). Shared TCR and BCRs between pre- and post-TCHP treatment of preliminary experiment were searched in main experiment (**Figure 1**).

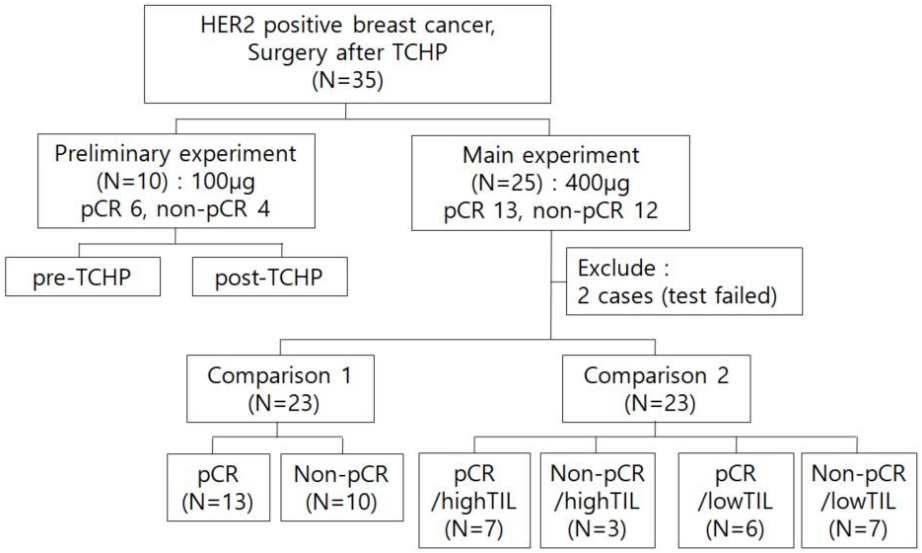

Figure 1. Schema of the study. Ten cases are allocated for preliminary experiment using 100μg of RNA, and remained twenty-five cases are main experiment using 400μg of RNA. Two cases of main experiment are excluded due to failure of immune repertoire assessment. In the comparison 1, immune repertoire is compared according to TCHP response, and in the comparison 2, the groups are subdivided according to the level of TILs, and four groups are compared.

2.2. Methods

2.2.1 Immunohistochemistry and silver in situ hybridization

Immunohistochemical (IHC) staining for estrogen receptor, progesterone receptor, HER2, and p53 were conducted in the core-needle biopsy of all cases and surgical specimen of non-pCR group. The antibody information is summarized on **Table 1.**

All IHC stainings were conducted on unstained 4μm thick formalin fixed paraffin embedded (FFPE) tissue sections, which were deparaffinized and re-hydrated by immersion in xylene and a graded ethanol series. Endogenous peroxidase was blocked by incubation in 3% H_2O_2 for 10 minutes, followed by heat-induced antigen retrieval. IHC labeling was performed using an autostainer (Benchmark XT; Ventana Medical Systems, Tucson, AZ, USA) according to the manufacturer's protocol. Briefly, sections were incubated at room temperature for 24 or 32 minutes with primary antibodies and then washed. An ultraView AP Magenta Detection Kit (Ventana Medical Systems) was used for magenta chromogen, and the OptiView DAB Detection Kit (Ventana Medical Systems) was used for the brown chromogen. Immunolabeled sections were lightly counterstained with hematoxylin, dehydrated in ethanol, and cleared in xylene. The immune-labeled slides were reviewed by two pathologists.

Automated silver in situ hybridization (SISH) assays were performed with INFORM HER2 DNA and chromosome 17 probes (Ventana Medical Systems) at the 4μm tissue section of HER2 2+ cases, using an ultraView SISH Detection Kit (Ventana Medical Systems) according to the manufacturer's protocols. Both probes are prelabeled with dinitrophenol (DNP) and the HER2 DNA probe was denatured at 80˚C for 12 minutes. Hybridization was performed at 44˚C for 6 hours, followed by three washes at 72˚C. The chromosome 17 probe was denatured at 80˚C for 12 minutes, and hybridization was performed at 44˚C for 6 hours on the same slide, followed by three washes at 72˚C. The probes were visualized using a rabbit anti-DNP primary antibody and goat anti-rabbit antibody conjugated to horseradish peroxidase as the chromogenic enzyme. The silver precipitate was deposited in the

nuclei after sequential addition of silver acetate, hydroquinone, and H_2O_2, and single copy of the *HER2* gene was seen as a black dot. A red dot for chromosome 17 appeared following a reaction with fast red and naphthol phosphate. The specimens were then counterstained with Harris hematoxylin.

Table 2. Antibodies information for IHC stainings

Antigens	Antibodies	Clones	Dilutions	Manufacturer
Estrogen receptor	Mouse monoclonal	6F11	1:200	Novo Castra (Newcastle, UK)
Progesterone receptor	Mouse monoclonal	PGR-312	1:200	Novo Castra (Newcastle, UK)
HER-2 (C-ERB B2)	Rabbit monoclonal	4B5	1:8	Ventana (Tucson, USA)
p53	Mouse monoclonal	DO-7	1:1000	Dako (Glostrup, Denmark)

2.2.2. Pathologic evaluation

All of the pre-treatment core-needle biopsy and the surgical specimen were reviewed. On the core-needle biopsy, stromal TILs and nuclear and histologic grade of the breast carcinoma were evaluated. The level of TILs was expressed as a percentage according to instruction by International TIL Working Group (5). Residual cancer burden (RCB) score, Miller-Payne grade, residual tumor size, and TILs were reviewed on the surgical specimen (11, 12). In the cases of pCR group, tumor bed area (the area with the stromal reaction) was marked and collected for the high-throughput NGS.

2.2.3. High-throughput sequencing for immune repertoire

The selected area of FFPE tissue of the preliminary experiment were obtained with microtome in 5μm thickness, and AllpreRNA FFPE kit (Qiagen, Hilden, Germany) was used for the RNA extraction of the preliminary experiment, according to the manufacture's instruction. All samples of main experiment were extracted with Maxwell RSC RNA FFPE kit (Promega, Madison, USA), according to the manufacture's instruction on a Maxwell RSC device from Promega. All of the RNA samples were quantified in fluorescence using QuantiTdsDNA assay kits (Invitrogen, Waltham, USA).

For the library construction, 100μg for preliminary experiment and 400μg for main experiment of RNA was used as input of library generation with the immunoverse^{TM}-HS TCR alpha/delta/beta/gamma Kit, BCR IGH/K/L kit (DB0219 and DB0221 Archer, Zaragoza, Spain) according to the manufacturer's instruction. The intended concentration of pooled libraries was confirmed with Collibri library quantification kit (Thermo Fisher Scientific, Waltham, USA). Libraries were sequenced on an Illumina NextSeq 500 using NextSeq 500v2 reagents (Illumina, San Diego, Ca, USA) for paired end, 150 base pair (bp) reads, and dual index reads. Libraries were multiplexed, and the concentration of the sample library was calculated from the standard curve.

The Illumina sequencer generated raw images utilizing sequencing control

software for system control and base calling through an integrated primary analysis software called Real Time Analysis. The base calls binary was converted into FASTQ utilizing illumine package bcl2fastq. Adapters were not trimmed away from the reads.

2.2.4. Data analysis for immune repertoire

Data was analyzed by Archer Analysis Immunoverse version 6.0. (ArcherDX). Briefly, adapter sequences were trimmed from the reads, and then, PCR duplicates were collapsed using molecular barcodes. Consensus reads representing unique input molecules were passed to MiXCR for V-(D)-J segment mapping and clonotype assembly.

The processed data were divided into productive and non-productive TCR and BCR, depending on whether the CDR3 sequences have a stop codon or sequences without matching amino acids.

2.2.5. Total Omics Transcriptome analysis

The libraries were prepared for 151 bp paired-end sequencing using TrueSeq standed mRNA Sample Preparation Kit (Illumina, CA, USA). Namely, mRNA molecules were purified and fragmented from 1μg of total RNA using oligo magnetic beads. After sequential process of end repair, A-tailing and adapter ligation, cDNA libraries were amplified with PCR. Quality of these cDNA libraries was evaluated with the Agilent 2100 BioAnalyzer (Agilent, CA, USA). They were quantified with the KAPA library quantification kit (Kapa Biosystems, MA, USA) according to the manufacturer's library quantification protocol. Following cluster amplification of denatured templates, sequencing was progressed as paired-end (2x151 bp) using Illumina NovaSeq6000 (Illumina, CA, USA).

The adapter sequences and the ends of the reads less than Phred quality score 20 were trimmed and simultaneously the reads shorter than 50 bp were removed by using cutadapt v.2.8. And the filtered reads were mapped to the reference genome related to the species using the aligner STAR v.2.7.1a, following ENCODE

standard options with "-quantMode TranscriptomeSMA" option for estimation of transcriptome expression level.

2.2.6. Data from published papers

We used databases of TCRdb (13), TCR3d (14), and vdjdb (15) for finding HER2 and mutant p53 (R175H, Y220C, G245S, and R248W) targeting TCR sequences (downloaded in 2019) (16). These sequences were compared with current study results, and sequences with substitution of 1 or 2 amino acids were considered as similar sequences (17, 18).

2.2.7. Analysis of differentially expressed genes and ontology

Transcript assembly and abundance estimation were performed to get the gene expression level. To remove the low expressed genes, we selected the genes with at least ten counts. After the selection of genes with threshold of absolute fold-change ≥ 1.5 and p-value < 0.05, a hierarchical clustering heatmap was performed using heatmap package in R. We estimated the activation of the hallmark pathways associated with treatment response and immune repertoire by performing several steps. First, Pearson correlation coefficient was calculated between each RNA expression and immune repertoire profiles. Second, lists of genes with positive correlation > 0.5 or negative correlation < -0.5 were selected. Third, hallmark pathway analysis was conducted using DAVID Bioinformatics Resources 6.8. A q-value of < 0.05 was considered significant.

2.2.8. Cell-type Identification by Estimating Relative Subtypes of RNA Transcripts (CIBERSORT)

CIBERSORT is a decovolution method that has been validated on gene expression profile which referred to as "digital cytometry" (19). RNA expression data was uploaded to the cell-type identification by estimating relative subtypes

(CIBERSORT) web portal (https://cibersort.stanford.edu/), and the results was downloaded.

2.2.9. PAM50 subtypes and gene expression data

Expression of the genes of prediction analysis of microarray 50(PAM50) were normalized, and standardized to five housekeepers, according to the standard practice (20). The published PAM50 algorithm was used to classify each cases into the subtypes: luminal A, luminal B, basal-like, Her2-enriched, normal- like and not applicable (NA).

2.2.10 Statistical analysis

Immune repertoire was evaluated in following aspects: richness, density, Shannon's entropy index (SDI), length of amino acid, and composition. Richness was total number of the separate clones, defined by the same V, D, and J usage and CDR3 sequences. Density was sum of each clonal count. Shannon's entropy index was calculated by the following equation: $H' = -\sum_{i=1}^{R} p_i \ln p_i$($H'$ = SDI, R=the number of separate clones, p = the proportion of each clone). Length of amino acid was measured by counting the number of amino acids consisting CDR3 of the TCR or BCR. Composition was groups divided by the proportion of each clone occupying in its entire clone count.

For the comparison, Mann-Whitney test was used to compare the mean values of each group, and Chi-square or Fisher's exact test was conducted to compare the proportion of each group. On the preliminary experiment, pre- and post-TCHP groups were compared with pair-wise t test. Pearson correlation coefficient was calculated to evaluate the relationship between RCB score and immune repertoires.

On the main experiment, sequences with a significantly high frequency in pCR group was selected, and the principal component analysis (PCA) was performed by obtaining the relative distance through the Levenshtein distance. False discovery rate

(FDR) correction was applied to correct for type 1 error due to multiple comparisons. For all analyses, p-value or q-value of < 0.05 was considered statistically significant. All data were analyzed using R Statistical Software (version 3.6.1).

3. Results

3.1. Clinicopathologic characteristics of entire cases

Total 35 cases were assigned on the preliminary and the main experiment. **Table 2** summarizes the clinicopathologic characteristics of the preliminary and the main experiment. Only TIL and RCB score were significantly different in both experiments, TIL was higher in the preliminary experiment (preliminary experiment, mean 13%, and main experiment, mean 7%, $p = 0.008$) and RCB score was higher in main experiment (preliminary experiment, mean 0.471; main experiment mean 1.020, $p = 0.045$). The other characteristics showed no significant difference.

Table 3. Clinicopathologic characteristics of preliminary and main experiments

	Preliminary experiment (n=10)	Main experiment (n=25)	*p*-value
Age (median, range)	58 (46-65)	51 (32-71)	0.052
Tumor size (mean ±Std[1])	2.9±1.0	4.0±2.1	0.062
TIL[2] (%), (mean, ±Std)	13±16	7±9	**0.008***
RCB[3] class (%)			0.572
pCR[4]	6 (60)	13 (52)	
1	2 (20)	5 (20)	
2	2 (20)	3 (12)	
3	0 (0)	4 (16)	
RCB[5] score (mean, ±Std)	0.471±0.630	1.020±1.359	**0.045***
Histologic grade (%)			0.445
1	0 (0)	0 (0)	
2	7 (70)	14 (56)	
3	3 (30)	11 (44)	
Hormonal receptor (%)			
Negative	7 (70)	15 (66)	0.580
Positive	3 (30)	10 (33)	
Lymph node metastasis (%)	2 (20)	5 (20)	0.792

[1]Std, standard deviation, [2]TIL, tumor infiltrating lymphocyte; [3]RCB, residual cancer burden.[4]pCR, pathologic complete response; [5]RCB, residual cancer burden; **p*-value < 0.05

3.2. Changes of immune repertoire after TCHP treatment

Ten cases of the preliminary experiment were used to compare T cell and B cell repertoires before and after TCHP treatment. Characteristics of immune repertoire of both groups were summarized in **Table 3** and **4**. In TRA and TRB, most of the SDI, density, and richness were significantly decreased after treatment (SDI of TRA, $p = 0.037$ and TRB, $p = 0.037$; density of TRA, $p = 0.047$ and TRB, $p = 0.022$; richness of TRA, $p = 0.041$), but only the decrease in the richness of TRB was not statistically significant ($p = 0.053$). Length of CDR3 was similar in before and after TCHP treatment (TRA, $p = 0.918$ and TRB, $p = 0.308$). The clones occupying large proportion (1~ 10% and 0.1~ 1%) of both TRA and TRB were significantly increased after TCHP treatment ($p < 0.001$) (**Table 3**). In BCR, SDI of IGH, IGL, and IGK was increased, while density of IGH was decreased after treatment (SDI of IGH, $p = 0.014$, IGL, $p = 0.024$, and IGK, $p = 0.006$; density of IGH, $p = 0.006$). However, richness of IGH, IGL, and IGK, and density of IGL and IGK showed no significant change. In the aspect of the proportion of each class of immunoglobulin, IGHA was significantly decreased after the TCHP treatment ($p = 0.004$) with decrease of IGHA1/IGHA2 ratio ($p < 0.001$). In the IGHG subclass, IGHG2 was increased after TCHP treatment (pre-TCHP 20.4% and post-TCHP 27.9%; $p = 0.023$), and IGHG4 was decreased (pre-TCHP, 2.2% and post-TCHP 1.0%, $p = 0.023$). In light chain (IGL and IGK), the length of CDR3 was decreased significantly after TCHP treatment (IGL, $p = 0.024$, and IGK, $p = 0.006$), but there was no difference in heavy chain (IGH). After TCHP treatment, the composition of 1~10% and 0.1~1% clones was consistently increased in IGH, IGK, and IGL, which was statistically significant ($p < 0.001$) (**Table 4**). In pre-TCHP, richness of TRD and TRG was less than 10 in 40% of cases, and in post-TCHP, 70%. These results were not statistically comparable because it was difficult to interpret that the sequencing was successful. To supplement these results the input RNA was increased to 400μg in the main experiment.

The significant decrease of density, richness, and SDI were observed in both TRA and TRB, regardless of TCHP response. In BCR, density and richness of

IGH, IGK, and IGL were significantly decreased, however, SDI of IGH, IGK, and IGL was increased after TCHP treatment in both pCR and non-pCR groups (**Figure 2**).

Table 4. TRA and TRB repertoire in pre- and post-TCHP

		Pre-TCHP[1]	Post-TCHP[2]	*p*-value
SDI[3] (mean)				
TRA		5.4568	4.5545	**0.037***
TRB		6.5651	5.7371	**0.037***
Density (mean)				
TRA		7,890	1,728	**0.047***
TRB		45,289	8,738	**0.022***
Richness (mean)				
TRA		1,880	281	**0.041***
TRB		5,779	1,062	0.053
Length of CDR3 (mean)				
TRA		13.6	13.2	0.918
TRB		15.7	15.4	0.308
Composition (mean)				
TRA	1~10%	9 (0.5%)	15 (5.3%)	**< 0.001***
	0.1~1%	162 (8.6%)	186 (66.2%)	
	0.01~0.1%	651 (34.6%)	80 (28.5%)	
	< 0.01%	1058 (56.3%)	0 (0%)	
TRB	1~10%	5 (0.1%)	6 (0.6%)	**< 0.001***
	0.1~1%	170 (2.9%)	183 (17.2%)	
	0.01~0.1%	990 (17.1%)	732 (68.9%)	
	< 0.01%	4615 (79.9%)	141 (13.3%)	

[1]Pre-TCHP, needle biopsy specimen before TCHP treatment; [2]post-TCHP, surgical specimen after TCHP treatment; [3]SDI, Shannon diversity index; **p*-value <0.05

Table 5. BCR repertoire in pre- and post-TCHP

	Pre-TCHP[1]	Post-TCHP[2]	*p*-value
SDI[3] (mean)			
IGH	5.882	6.820	**0.014***
IGL	4.910	5.897	**0.024***
IGK	5.269	7.412	**0.006***
Density (mean)			
IGH	172,095	36,327	**0.006***
IGL	56,087	5,837	0.249
IGK	318,129	79,613	0.249
Richness (mean)			
IGH	9,906	4,476	0.153
IGL	2,966	1,061	0.153
IGK	9,710	7,023	0.918
Length of CDR3 (mean)			
IGH	21.6	21.8	0.475
IGL	18.2	11.8	**0.024***
IGK	17.3	14.6	**0.006***
Richness, classes and subtypes (mean)			
IGHM	1181 (11.9%)	681 (15.2%)	0.100
IGHD	96 (1.0%)	20 (0.5%)	0.285
IGHA	1814 (18.3%)	1642 (36.7%)	**0.004***
IGHA1	1398 (77.1%)	935 (56.9%)	**< 0.001***
IGHA2	413 (22.8%)	707 (43.1%)	**< 0.001***
Indeterminate	3 (0.1%)	0 (0%)	0.053
IGHG	6779 (68.4%)	2128 (47.5%)	**0.003***
IGHG1	4382 (64.6%)	1339 (62.9%)	0.051
IGHG2	1288 (19.0%)	576 (27.1%)	**0.023**
IGHG3	491 (7.1%)	131 (6.2%)	0.282
IGHG4	147 (2.2%)	22 (1.0%)	**0.023***
Indeterminate	471 (6.9%)	61 (2.8%)	**0.006***
Indeterminate	37 (0.4%)	6 (0.1%)	0.051

Composition (mean)				
IGH	1~ 10%	138 (0.1%)	195 (0.1%)	**< 0.001***
	0.1~ 1%	1,231 (1.2%)	1,443 (3.2%)	
	0.01~ 0.1%	5,740 (5.8%)	14,580 (32.6%)	
	0.001~ 0.01%	34,141 (34.5%)	28,685 (64.1%)	
	< 0.001 %	57,812 (58.4%)	0 (0%)	
IGK	1~10%	155 (0.2%)	39 (0.1%)	**< 0.001***
	0.1~ 1%	984 (1.2%)	1,121 (1.6%)	
	0.01~ 0.1%	5,282 (6.7%)	18,981 (27.0%)	
	0.001~ 0.01%	24,258 (30.7%)	38,338 (54.6%)	
	< 0.001 %	48,424 (61.2%)	11,757 (16.7%)	
IGL	1~10%	165 (0.5%)	99 (0.9%)	**< 0.001***
	0.1~ 1%	1,031 (3.5%)	2,002 (18.9%)	
	0.01~ 0.1%	4,603 (15.5%)	7,746 (73.0%)	
	0.001~ 0.01%	11,949 (40.3%)	765 (7.2%)	
	< 0.001%	11,910 (40.2%)	0 (0%)	

[1]Pre-TCHP, needle biopsy specimen before TCHP treatment; [2]post-TCHP, surgical specimen after TCHP treatment; [3]SDI, Shannon diversity index; **p*-value <0.05

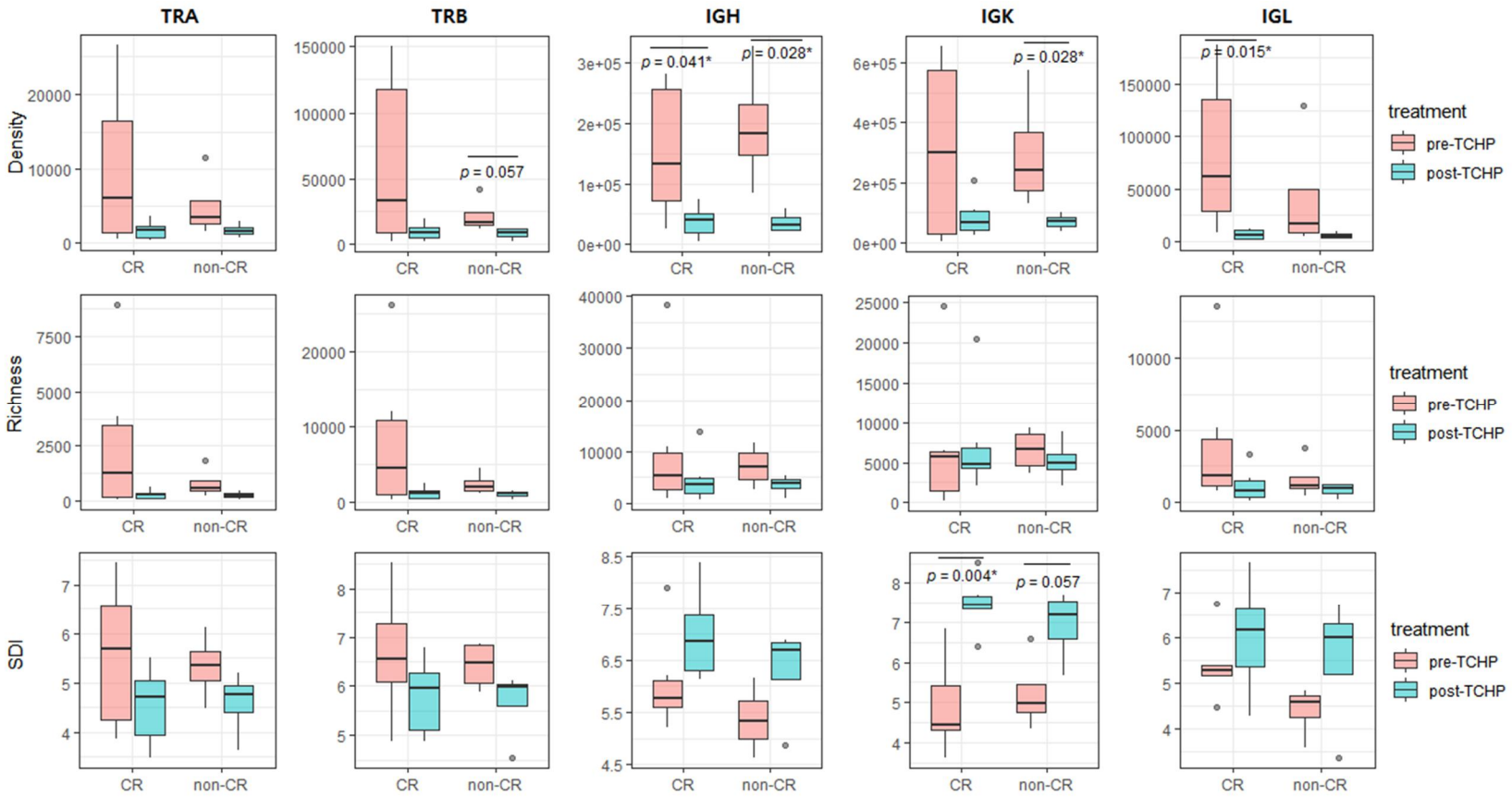

Figure 2. Pre- and post-TCHP immune repertoire according to TCHP response in preliminary experiment. Regardless of TCHP response, density and richness of TCR and BCR are decreased after the treatment. SDI tends to decrease in TCR and increase in BCR. Among them, IGK shows a statistically significant increase.

3.3. Immune repertoire according to the TCHP response

Main experiment included pre-TCHP biopsy samples of 25 patients, however, two cases were excluded from analysis because amplification did not occur during the sequencing process. The remained 23 cases were composed of 13 cases of pCR group, and 10 cases of non-pCR group. In the main experiment, the clinicopathologic characteristics grouped by TCHP response were described in **Table 5**. When comparing the pCR and non-pCR groups, all of the characteristics did not show significant association with response to TCHP.

Table 6. Clinicopathologic characteristics in main experiment

	pCR[1] (n=13)	Non-pCR[2] (n=10)	*p*-value
Age (median, range)	51 (38-67)	52 (32-71)	0.563
Tumor size (mean ± Std[3])	3.7 ± 1.7	4.5 ± 2.7	0.483
TIL[4] (%), (median, range)	10 (0-20)	0 (0-30)	0.563
RCB[5] class			NA
0	13 (100%)	0 (0%)	
1	0 (0%)	3 (30%)	
2	0 (0%)	3 (30%)	
3	0 (0%)	4 (40%)	
RCB score (median, range)	0 (0)	1.187 (0.889-1.446)	NA
HG[6] (cases)			0.376
1	0 (0%)	0 (0%)	
2	5 (38%)	5 (50%)	
3	8 (62%)	5 (50%)	
LN[7] metastasis (%)	0 (0%)	5 (50%)	
Hormonal receptor (cases) (%)			0.376
Negative	9 (70%)	4 (40%)	
Positive	4 (30%)	6 (60%)	
HER2 3+	12 (92%)	7 (70%)	0.162

[1]pCR, pathologic complete response; [2]non-pCR, non-pathologic complete response; [3]Std, standard deviation; [4]TIL, tumor infiltrating lymphocytes; [5]RCB, residual cancer burden; [6]HG, histologic grade; [7]LN, lymph node.

In TCR, mean of TRA, TRB, TRD, and TRG showed no significant difference in SDI, density, richness, and length of CDR3 according to TCHP response. The composition of the clones was significantly different in pCR and non-pCR groups ($p < 0.001$). The proportion of *TRGV9* and *TRDV2*, which represent Vγ9Vδ2 T cells, were not significantly different in pCR and non-pCR groups (**Figure 3, Table 6**). None of the characteristics of TRA and TRB repertoires were correlated with RCB score (**Figure 4**).

In BCR, IGH, IGK, and IGL showed no significant difference in SDI, density, richness, and length of CDR3. In immunoglobulin class, pCR group had more IgG (71.2%) than non-pCR group (63.3%), but it was not statistically significant ($p = 0.052$). IgG subtypes showed similar distribution in both groups. In all of the IGH, IGK, and IGL, pCR and non-pCR groups showed significantly different composition ($p < 0.001$), but only $< 10^{-5}$ category of IGK showed more a difference more than 10%, pCR group was 37.0% and non-pCR group was 27.0%. Totally, sixty-three clones of hypermutated IGH were reported. Mean of the richness was 2.5 clones in pCR and 2.8 clones in non-pCR. On the other hand, mean of density of hypermutated IGH were 87,794 in pCR group and 101,330 in non-pCR group. Density, richness, and frequency of hypermutated IGH were not significantly different between pCR and non-pCR groups (**Figure 5, Table 7**). None of the characteristics of BCR repertoires were correlated with RCB score (**Figure 6)**.

Table 7. TCR repertoires according to TCHP response in main experiment

		pCR[1] (n=13)	Non-pCR[2] (n=10)	*p*-value
SDI[3] (mean)				
TRA		6.797	6.629	0.131
TRB		6.802	6.635	0.232
TRD		3.714	3.756	0.131
TRG		2.510	2.462	0.232
Density (mean)				
TRA		15,426	15,087	0.831
TRB		59,895	56,654	0.738
TRD		407	483	0.756
TRG		350	431	0.605
Richness (mean)				
TRA		4,194	3,284	0.446
TRB		9,862	7,902	0.41
TRD		150	146	0.852
TRG		128	119	0.852
Length of CDR3 (mean)				
TRA		14.2	13.5	0.278
TRB		16.3	16.4	0.556
TRD		19.4	19.5	0.784
TRG		14.0	13.7	0.284
Frequency of top 1% clone (%)				
TRA		15.5	15.6	0.975
TRB		25.8	25.7	0.975
Composition†(%)				
TRA	1 ~ 10 %	2.2 (0.1%)	2.1 (0.1%)	**< 0.001** *
	0.1~ 1 %	119.5 (2.9%)	120.6 (3.7%)	
	0.01~ 0.001 %	2,125 (50.7%)	1,921.1 (58.5%)	
	< 0.001 %	1947.4 (46.4%)	1,240.7 (37.8%)	
TRB	1~ 10 %	3.2 (0.1%)	3.1 (0.1%)	**< 0.001** *
	0.1~ 1 %	111.2 (1.1%)	112.0 (1.4%)	

0.01~ 0.001 %	1,396.2 (14.2%)	1,712.0 (22.7%)	
< 0.001 %	13,890.6 (84.7%)	6,075.6 (76.9%)	
TRG subtypes (%)			0.614
TRGV9	29 (22.5%)	30 (25.2%)	
Others	100 (77.5%)	89 (74.8%)	
TRD subtypes (%)			0.107
TRDV2	56 (37.3%)	68 (46.5%)	
Others	94 (62.7%)	78 (53.4%)	

[1]pCR, pathologic complete response; [2]non-pCR, non- pathologic complete response; [3]SDI, Shannon diversity index; *p-value < 0.05

Table 8. BCR repertoires according to the TCHP response in main experiment

	pCR[1] (n=13)	Non-pCR[2] (n=10)	p-value
SDI[3] (mean)			
IGH	6.043	6.144	0.562
IGK	5.902	6.213	0.748
IGL	5.224	5.631	0.519
Density (mean)			
IGH	703,501	615,449	0.519
IGK	766,938	594,411	0.365
IGL	221,145	171,358	0.439
Richness(mean)			
IGH	17,160	15,257	0.949
IGK	10,713	10,673	0.748
IGL	5,025	4,626	1.000
Length of CDR3 (mean)			
IGH	21.8	21.5	0.089
IGK	16.1	16.4	0.060
IGL	14.1	13.1	0.143
Richness, each subtype (mean)			

IGHM		1,225 (7.3%)	1,442 (9.1%)	0.286
IGHD		140 (0.8%)	123 (0.8%)	0.705
IGHA		3,434 (20.6%)	4,227 (26.8%)	0.113
IGHA1		2,214 (64.5%)	2,516 (64.8%)	0.868
IGHA2		1,217 (35.4%)	1,363 (35.1%)	0.875
Indeterminate		3 (0.1%)	3 (0.1%)	0.760
IGHG		11,884 (71.2%)	10,002 (63.3%)	0.052
IGHG1		7,715 (64.9%)	5,329 (60.5%)	0.189
IGHG2		2,528 (21.3%)	2,121 (24.1%)	0.156
IGHG3		908 (7.6%)	822 (9.3%)	0.358
IGHG4		247 (2.6%)	185 (2.1%)	0.866
Indeterminate		487 (4.1%)	350 (4.0%)	0.673
Indeterminate		6 (0.0%)	5 (0.0%)	0.641
Composition† (mean)				
IGH	1~ 10 %	10.2 (0.1%)	13.4 (0.1%)	**< 0.001***
	0.1~ 1 %	100.3 (0.7%)	119.3 (0.6%)	
	0.01~ 0.1 %	720.3 (4.7%)	1,049.7 (5.7%)	
	0.001~ 0.01 %	3,572.3 (23.2%)	4,662.2 (25.3%)	
	< 0.001 %	11,007.8 (71.4%)	12,578.7 (68.3%)	
IGK	1~ 10 %	10.6 (0.1%)	13.6 (0.1%)	**< 0.001***
	0.1~ 1 %	100.7 (1.1%)	119.8 (1.0%)	
	0.01~ 0.1 %	836.5 (8.7%)	1,237.9 (9.9%)	
	0.001~ 0.01 %	2,647.6 (27.6%)	3,723 (30.0%)	
	< 0.001 %	5,986.7 (62.5%)	7,417.2 (59.3%)	
IGL	1~ 10 %	12.4 (0.3%)	13.4 (0.2%)	**< 0.001***
	0.1~ 1 %	83.6 (1.8%)	117.4 (2.1%)	
	0.01~ 0.1 %	640.1 (14.1%)	1,116.7 (20.1%)	
	0.001~ 0.01 %	2128.7 (46.8%)	2,816 (50.6%)	

< 0.001 %	1684.2 (37.0%)	1,496.8 (27.0%)	
Hypermutation			
Density (mean)	87,794	101,330	0.821
Richness (mean)	2.5	2.8	0.663
Frequency (mean)	11.2	13.3	0.711

[1]pCR, pathologic complete response; [2]non-pCR, non-pathologic complete response; [3]SDI, Shannon diversity index; **p*-value < 0.05

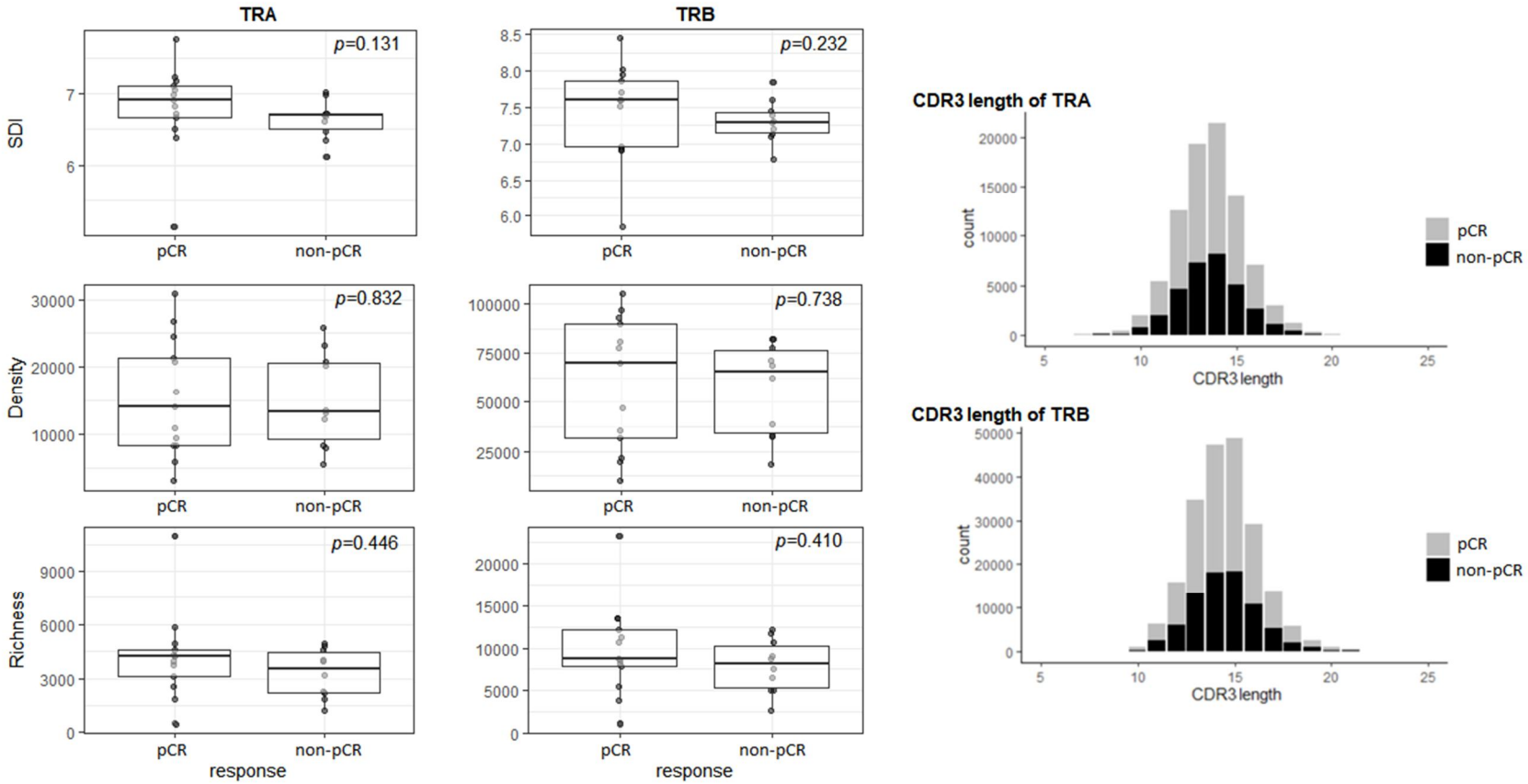

Figure 3. TCR repertoires according to the TCHP response in main experiment. SDI, density, richness and length of CDR3 of both TRA and TRB showed no significant difference between pCR and non-pCR groups

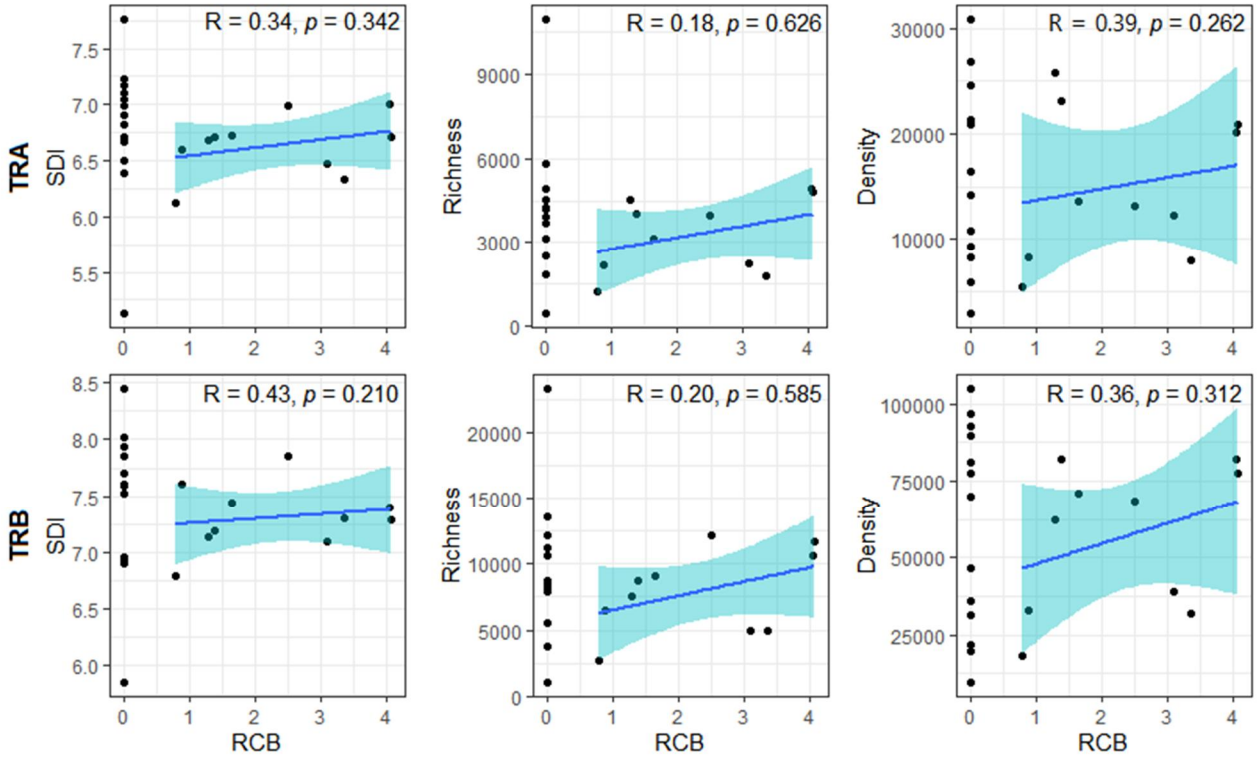

Figure 4. Correlation between TCR repertories and RCB score. None of SDI, richness and density of TCR were significantly associated with RCB score.

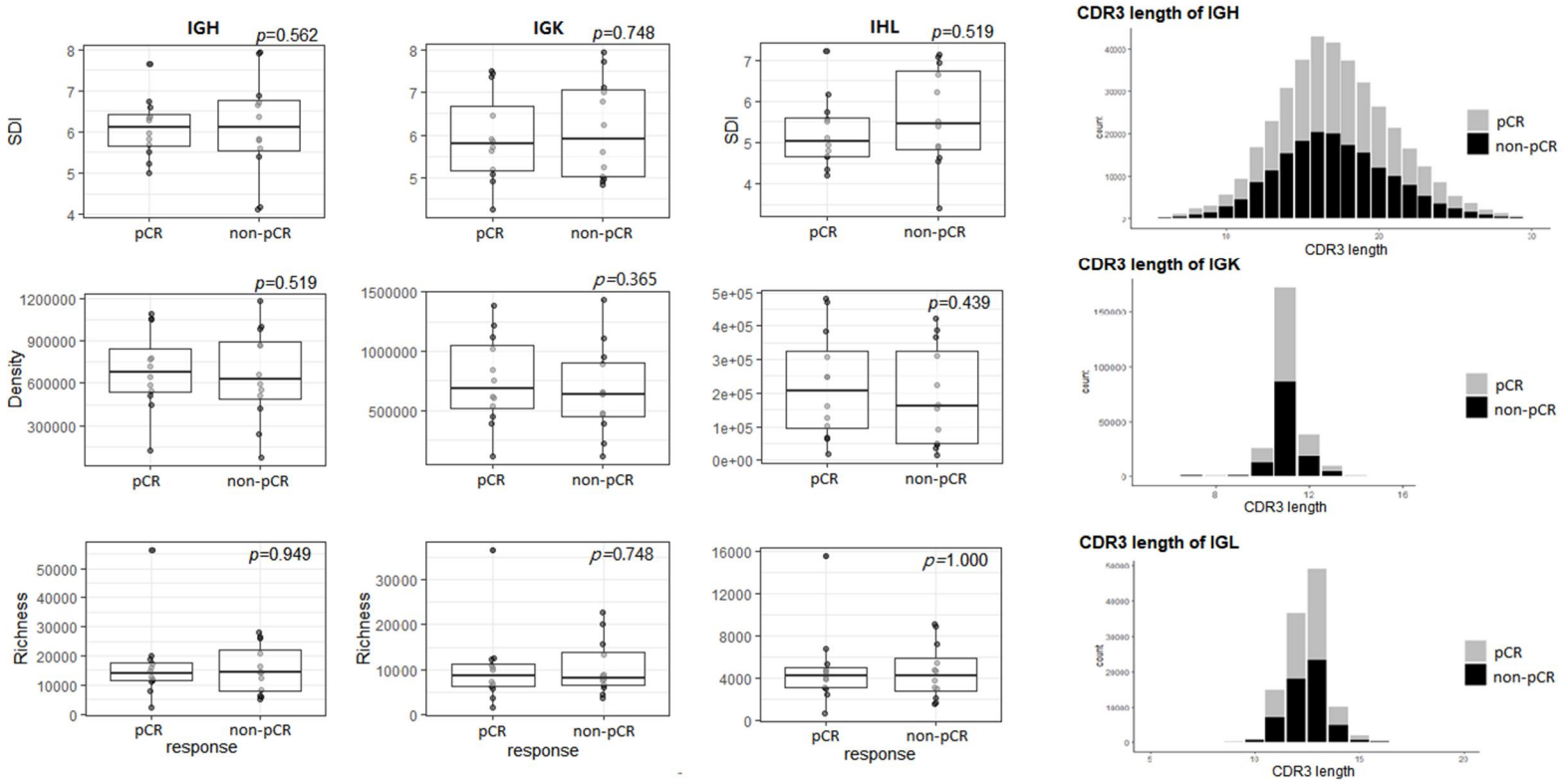

Figure 5. BCR repertoires according to the TCHP response in main experiment. SDI, density, richness and length of CDR3 of IGH, IGK and IGL showed no significant difference between pCR and non-pCR groups.

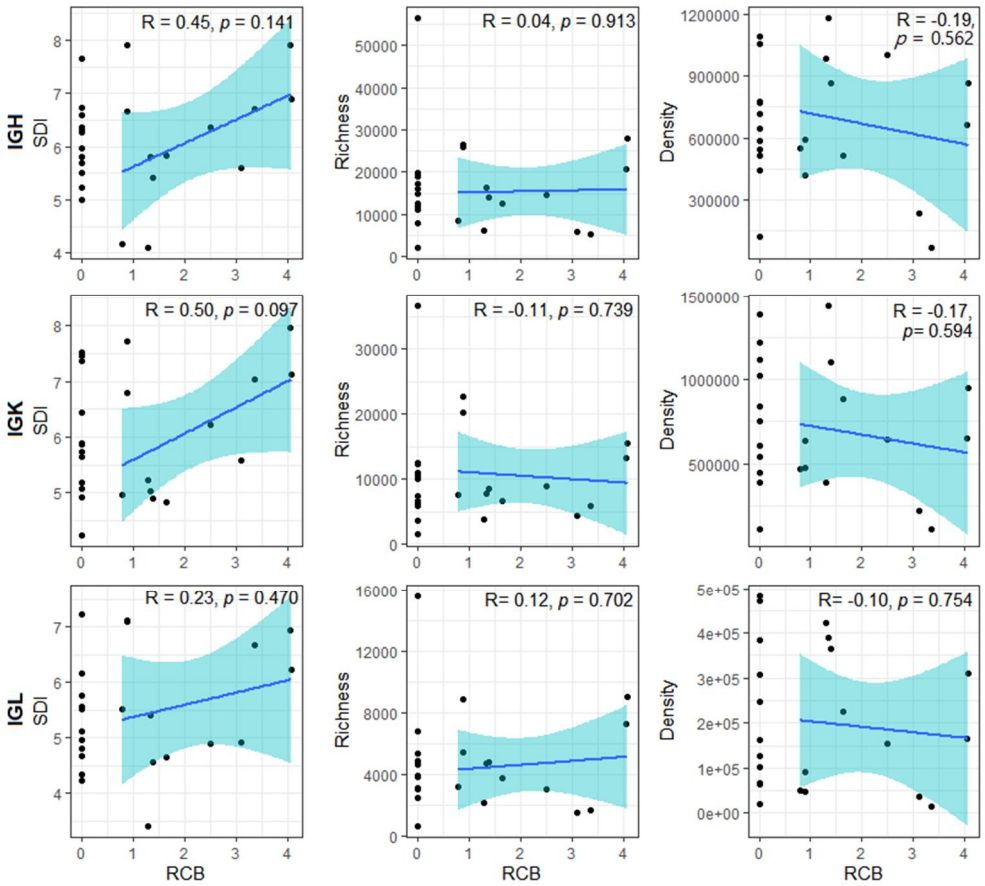

Figure 6. Correlation between BCR and RCB score. None of SDI, richness and density of BCR were correlation between RCB score.

3.4. V, D, and J usage of TRA and TRB according to the TCHP response

The usage of *V, D,* and *J* genes of TRA and TRB was compared according to the response to TCHP treatment. Regardless of pCR and non-pCR, most commonly used *TRAV* segment was *TRAV12-2,* followed by *TRAV13-1* and *TRAV9-2*. Only *TRAV34* showed the difference between pCR and non-pCR, but there was no statistical significance after correction of type 1 error ($p = 0.022$, $q = 0.735$). In TRAJ, most common segment of pCR is *TRAJ23* followed by *TRAJ39* and *TRAJ43*. In the order of frequency, *TRAJ43, TRAJ20,* and *TRAJ10* were the most commonly used in non-pCR. None of the TRAJ segment showed significant difference between pCR and non-pCR after type 1 error correction (**Table 8, Figure 7**). In TRB of pCR, *TRBV20-1, TRBV28,* and *TRBV7-9* were the most frequent segments, and in non-pCR, *TRBV18, TRBV6-1,* and *TRBV20-1* were used most commonly. In TRBD of both pCR and non-pCR, *TRBD1* was more common than *TRBD2*. In *TRBJ, TRBJ2-1* was most frequent, followed by *TRBJ2-7* and *TRBJ1-1* in both pCR and non-pCR, and significant difference between the two groups was not identified (**Table 8, Figure 8**).

In V-J gene paring of TRA, the most common V-J gene pair of pCR was *TRAV13-1/TRJ13, TRAV12-2/TRAJ3,* and *TRAV9-2/TRAJ54* in order of frequency (mean of frequency, *TRAV13-1/TRAJ13*, 0.4%; *TRAV12-2/TRAJ3*, 0.4%; and *TRAV9-2/TRAJ54* 0.3%). In non-pCR, *TRAV4/TRAJ34* was the most frequent pair, followed by *TRAV2/TRAJ10* and *TRAV1-2/TRAJ20* (mean of frequency, *TRAV4/TRAJ34*, 0.5%; *TRAV2/TRAJ10*, 0.5%; and *TRAV1-2/TRAJ20*, 0.4%). Sixty-three V-J gene pairs of TRA were differently expressed ($p < 0.05$) between pCR and non-pCR group, however, none of gene showed statistical significance in *q*-value (**Table 9**). In TRB, only 16 V-J pairs showed different expression between pCR and non-pCR group, none of which showed statistical difference after type 1 error correction (**Table 10**).

Table 9. List of top 10 the V(D)J segments of TRA and TRB in the order of frequency (%)

Gene	Segment	pCR[1] (n=10)	Non-pCR[2] (n=13)	*p*-value	*q*-value
TRA	*TRAV12-2*	5.8	5.9	0.961	0.899
	TRAV13-1	5.7	4.9	0.137	0.795
	TRAV9-2	4.7	4.0	0.221	0.795
	TRAV26-1	3.9	3.1	0.067	0.735
	TRAV21	3.8	3.8	0.918	0.899
	TRAV14DV4	3.6	3.3	0.554	0.899
	TRAV12-1	3.5	3.5	0.892	0.899
	TRAV29DV5	3.5	3.6	0.714	0.899
	TRAV12-3	3.4	3.2	0.489	0.894
	TRAV17	3.4	3.2	0.456	0.87
	*TRAV34***	0.4	0.2	**0.022***	0.735
	TRAJ23	3.15	2.73	0.286	0.795
	TRAJ39	3.08	2.55	**0.039***	0.735
	TRAJ43	2.95	3.14	0.699	0.899
	TRAJ45	2.93	2.81	0.631	0.899
	TRAJ10	2.87	2.99	0.807	0.899
	TRAJ4	2.84	2.75	0.838	0.899
	TRAJ49	2.83	2.63	0.404	0.851
	TRAJ37	2.7	2.58	0.645	0.899
	TRAJ20	2.67	3.13	0.26	0.795
	TRAJ54	2.6	2.22	0.092	0.795
TRB	*TRBV20-1*	8.54	7.73	0.263	0.795
	TRBV28	5.76	5.7	0.94	0.899
	TRBV7-9	4.48	4.66	0.694	0.899
	TRBV7-2	4.4	4.66	0.279	0.795
	TRBV5-1	4.37	5.04	0.187	0.795
	TRBV29-1	4.24	3.87	0.306	0.795
	TRBV6-5	3.98	3.11	0.365	0.809
	TRBV4-1	3.9	3.24	0.297	0.795
	TRBV19	3.88	3.71	0.7	0.899
	TRBV27	3.87	4.41	0.29	0.795
	D_ambiguous	31.84	32.63	0.876	0.899
	TRBD1	34.8	35.0	0.88	0.899
	TRBD2	28.1	26.5	0.084	0.795
	TRBJ2-1	19.97	19	0.469	0.876
	TRBJ2-7	18.72	18.62	0.094	0.795
	TRBJ1-1	16.3	15.55	0.474	0.876
	TRBJ2-3	8.79	10.35	0.063	0.735
	TRBJ2-5	8.12	8.92	0.321	0.809

	TRBJ1-5	5.73	5	0.211	0.795
	TRBJ2-2	5.22	4.49	**0.050***	0.735
	TRBJ1-2	4.24	3.94	0.467	0.876
	TRBJ1-6	2.45	2.54	0.771	0.899
	TRBJ1-4	2.36	2.86	**0.031***	0.735

[1]pCR, pathologic complete response; [2]non-pCR, non-pathologic complete response; **p*-value < 0.05
**Despite of *TRAV34* exceeded the 10th in frequency order, it is shown in the table, because the *p*-value is less than 0.05

Table 10. List of paired V-J usage of TRA with $p < 0.05$ between pCR and non-pCR

V	J	pCR[1]	Non-pCR[2]	*p*-value	*q*-value
TRAV13-1	*TRAJ10*	0.27	0.1	0.008	0.945
TRAV5	*TRAJ12*	0.03	0.08	0.037	0.945
TRAV25	*TRAJ13*	0.01	0.03	0.029	0.945
TRAV14DV4	*TRAJ15*	0.1	0.01	0.001	0.945
TRAV20	*TRAJ16*	0.08	0	0.007	0.945
TRAV10	*TRAJ20*	0.02	0.05	0.021	0.945
TRAV12-2	*TRAJ23*	0.34	0.19	0.030	0.945
TRAV26-2	*TRAJ26*	0.02	0	0.014	0.945
TRAV38-2DV8	*TRAJ26*	0.01	0.03	0.018	0.945
TRAV14DV4	*TRAJ27*	0.07	0.04	0.047	0.945
AMBIGUOUS	*TRAJ28*	0.02	0.05	0.015	0.945
TRAV17	*TRAJ28*	0.09	0.02	0.010	0.945
TRAV19	*TRAJ28*	0.13	0.03	0.004	0.945
TRAV9-2	*TRAJ28*	0.14	0.08	0.030	0.945
TRAV19	*TRAJ29*	0.02	0	0.009	0.945
TRAV1-1	*TRAJ3*	0.02	0	0.045	0.945
TRAV29DV5	*TRAJ3*	0	0.02	0.026	0.945
TRAV17	*TRAJ30*	0.03	0.11	0.032	0.945
TRAV21	*TRAJ30*	0.01	0.05	0.016	0.945
TRAV35	*TRAJ31*	0.05	0.01	0.015	0.945
TRAV16	*TRAJ32*	0.03	0	0.035	0.945
TRAV38-1	*TRAJ32*	0	0.02	0.011	0.945
TRAV6	*TRAJ33*	0.03	0.07	0.037	0.945
TRAV17	*TRAJ34*	0.05	0.07	0.047	0.945
TRAV12-1	*TRAJ35*	0.01	0.04	0.026	0.945
TRAV22	*TRAJ36*	0.03	0	0.041	0.945
TRAV27	*TRAJ36*	0.03	0	0.048	0.945
TRAV34	*TRAJ36*	0.01	0	0.018	0.945
TRAV19	*TRAJ37*	0.01	0.04	0.022	0.945
TRAV14DV4	*TRAJ38*	0.08	0.01	0.018	0.945
TRAV19	*TRAJ39*	0.11	0.02	0.023	0.945
TRAV22	*TRAJ39*	0.03	0	0.038	0.945
TRAV1-1	*TRAJ4*	0.08	0.02	0.048	0.945
TRAV13-2	*TRAJ4*	0.1	0.02	0.043	0.945
TRAV25	*TRAJ40*	0.03	0.07	0.008	0.945
TRAV5	*TRAJ40*	0.07	0.02	0.015	0.945
TRAV16	*TRAJ45*	0.01	0.03	0.038	0.945
TRAV27	*TRAJ45*	0.05	0.01	0.014	0.945
AMBIGUOUS	*TRAJ47*	0.03	0.01	0.050	0.945
TRAV26-1	*TRAJ47*	0.15	0.03	0.036	0.945

TRAV12-1	*TRAJ48*	0.02	0	0.045	0.945
TRAV8-4	*TRAJ48*	0.03	0.09	0.019	0.945
TRAV13-1	*TRAJ49*	0.19	0.09	0.018	0.945
TRAV27	*TRAJ49*	0.08	0.03	0.042	0.945
TRAV6	*TRAJ49*	0	0.05	0.012	0.945
TRAV8-3	*TRAJ49*	0.03	0.09	0.030	0.945
TRAV10	*TRAJ52*	0.03	0	0.048	0.945
TRAV29DV5	*TRAJ52*	0.17	0.12	0.049	0.945
TRAV9-2	*TRAJ53*	0.06	0.03	0.050	0.945
TRAV13-2	*TRAJ54*	0.05	0.02	0.043	0.945
TRAV26-2	*TRAJ54*	0.06	0.02	0.046	0.945
TRAV29DV5	*TRAJ54*	0.14	0.22	0.042	0.945
TRAV14DV4	*TRAJ56*	0.11	0.01	0.011	0.945
TRAV8-6	*TRAJ57*	0.06	0.21	0.047	0.945
TRAV29DV5	*TRAJ6*	0.03	0.01	0.023	0.945
TRAV21	*TRAJ7*	0.01	0.09	0.034	0.945
TRAV8-3	*TRAJ8*	0.13	0.02	0.029	0.945
TRAV8-3	*TRAJ9*	0.07	0.03	0.026	0.945

[1]pCR, pathologic complete response; [2]non-pCR, non-pathologic complete response.

Table 11. List of paired V-J usage with $p < 0.05$ between pCR and non-pCR

V	J	pCR[1]	Non-pCR[2]	*p*-value	*q*-value
TRBV1	TRBJ1-1	0.0000	0.0001	0.017	0.964
TRBV5-3	TRBJ1-5	0.0001	0.0000	0.018	0.964
TRBV5-6	TRBJ1-5	0.0003	0.0007	0.026	0.964
TRBV7-3	TRBJ2-1	0.0057	0.0036	0.049	0.964
AMBIGUOUS	TRBJ2-2	0.0042	0.0033	0.036	0.964
TRBV5-4	TRBJ2-2	0.0010	0.0005	0.049	0.964
TRBV7-3	TRBJ2-2	0.0035	0.0008	0.042	0.964
TRBV19	TRBJ2-4	0.0008	0.0002	0.012	0.964
TRBV20-1	TRBJ2-4	0.0015	0.0006	0.042	0.964
TRBV4-3	TRBJ2-4	0.0001	0.0000	0.035	0.964
TRBV27	TRBJ2-5	0.0019	0.0033	0.030	0.964
TRBV9	TRBJ2-5	0.0013	0.0024	0.030	0.964
TRBV19	TRBJ2-6	0.0008	0.0014	0.049	0.964
TRBV27	TRBJ2-6	0.0002	0.0005	0.014	0.964
TRBV3-1	TRBJ2-6	0.0001	0.0002	0.032	0.964
TRBV10-2	TRBJ2-7	0.0023	0.0008	0.002	0.964

[1]pCR, pathologic complete response; [2]non-pCR, non-pathologic complete response

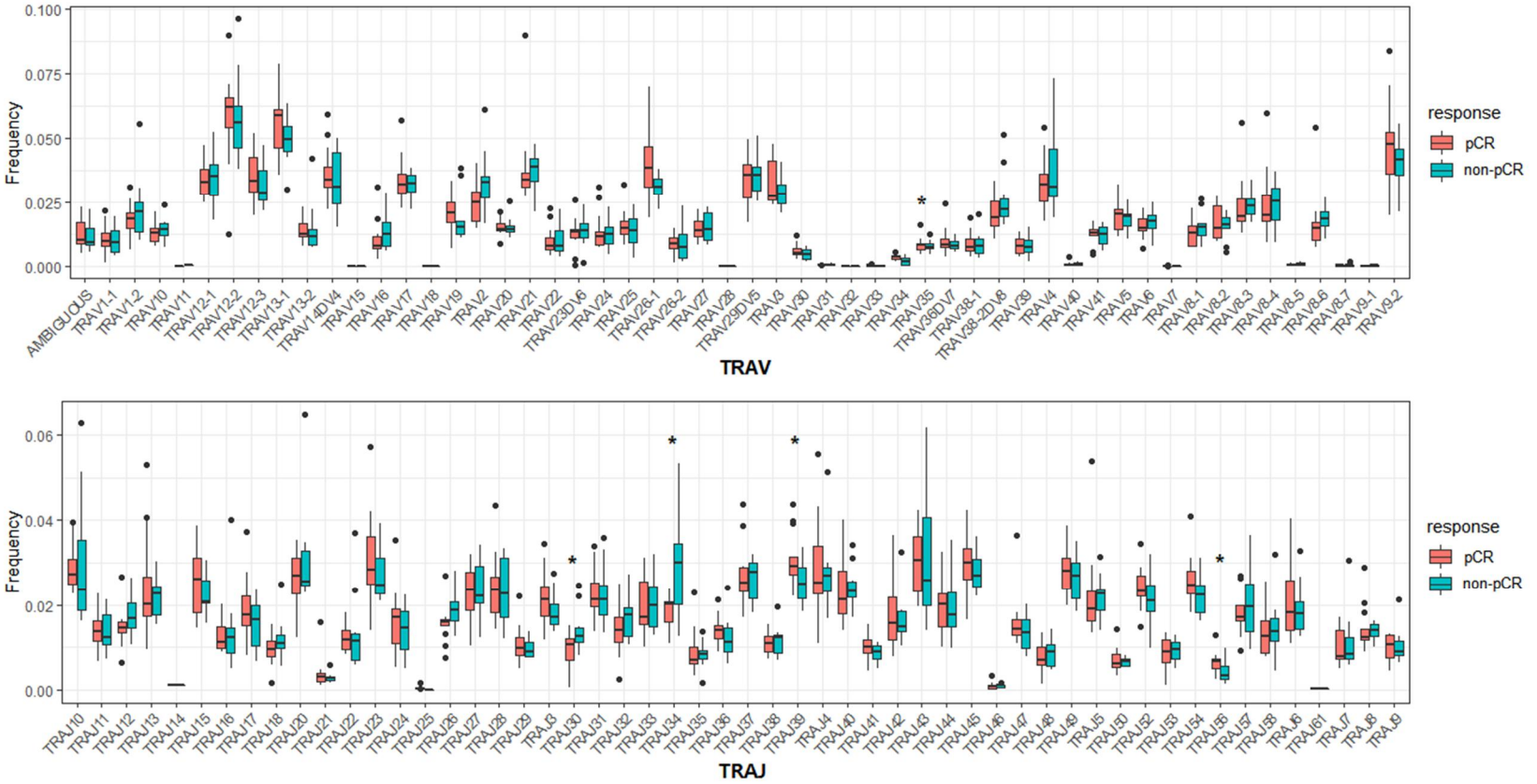

Figure 7. V- J usage of TRA according to TCHP response. A. TRAV usage. Only *TRAV34* showed *p*-value <0.05 but *q*-value is not significant. B. TRAJ usage. TRAJ30, TRAJ34, TRAJ39 and TRAJ56 showed *p*-value<0.05 but, *q*-value is not significant.

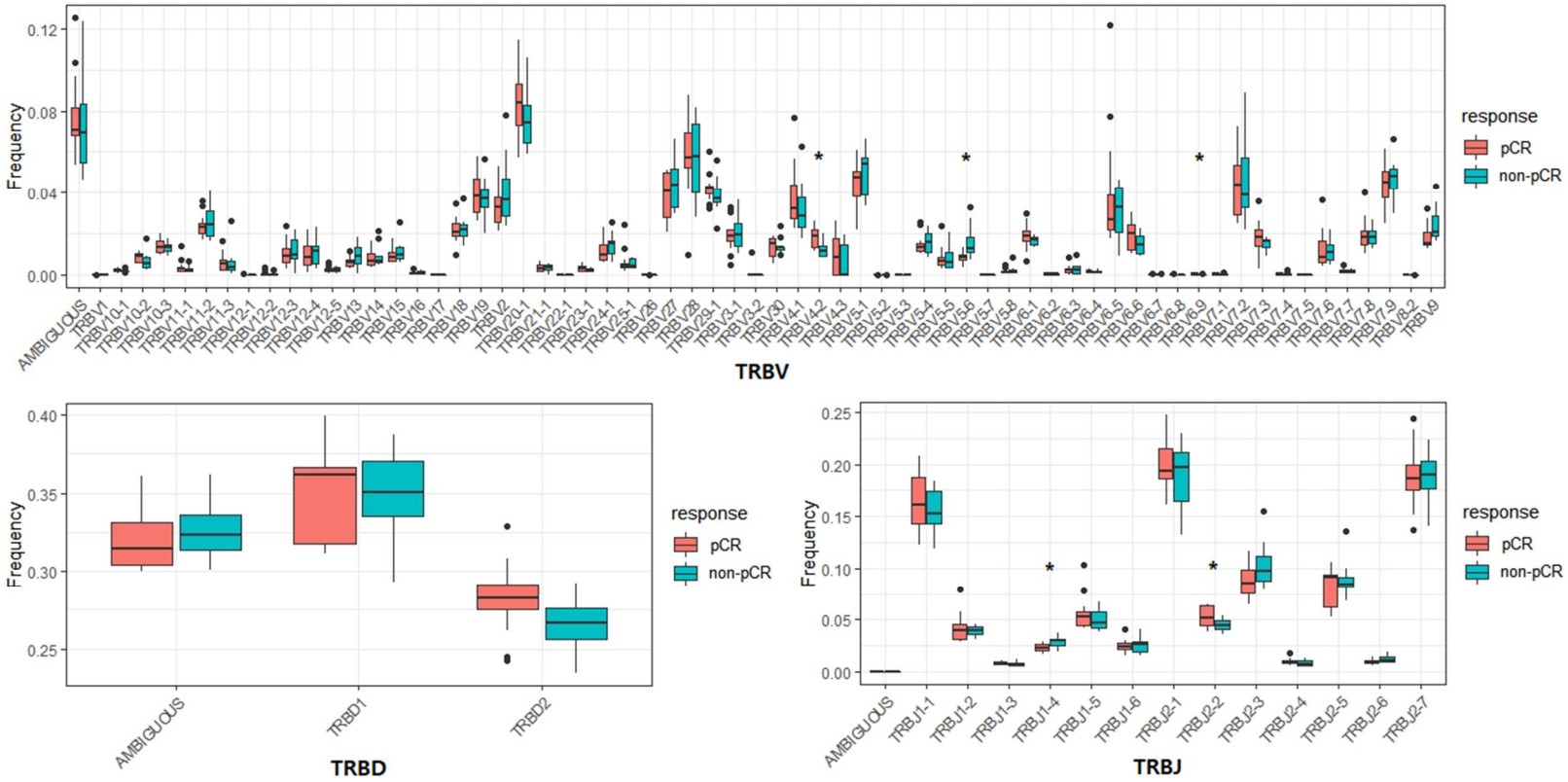

Figure 8. V-D-J usage of TRB according to TCHP response. A. TRBV usage according to TCHP response. TRBV4-2, TRBV5-6, and TRBV6-9 shows *p*-value <0.05, however *q*-value is not significant. B. TRBD usage. None of segment shows significant difference. C. TRBJ usage. TRBJ1-5 shows *p*-value <0.05, however, *q*-value is not significant.

3.5. MAIT according to the TCHP response

Classical MAIT is considered to have TCRα chain encoded by *TRAV1-2* with one of the J gene segment of *TRAJ33, TRAJ20, or TRAJ12*. We selected out the sequences using *TRAJ33, TRAJ20,* or *TRAJ12* with *TRAV1-2,* and 462 sequences were identified. Total density was 2,418, and mean of frequency was 0.2%. In both treatment response groups, mean of frequency, richness, and density showed no significant difference. The distribution of *TRAJ33, TRAJ20,* and *TRAJ12* were also similar in pCR and non-pCR groups (**Table 11, Figure 9A**).

In TRB, the clones encoded by *TRBV6* or *TRBV20* gene family members were also compared in pCR and non-pCR group, because classical MAIT preferentially pairs TCRβ encoded by *TRBV6* or *TRBV20* gene family member. Totally, 28,782 clones were identified from the TRB of which the density was 199,504 and mean of frequency was 14.0%. When compared according to TCHP treatment response, the mean of density, richness, and frequency were consistently higher in pCR than non-pCR groups, however, statistically not significant. In both groups, *TRBV20* was more frequent and abundant than *TRBV6* gene family (**Table 11, Figure 9B**).

Up to a quarter of TRB of MAIT is encoded by up *TRBV* other than *TRBV6* or *TRBV20* family members (17). Therefore, we searched out MAIT sequences in TCRdb, and 12,879 TRBs were downloaded. Two hundred one clones were extracted from TRB of current study, of which V, D, and J gene segments and CDR3 amino acids were the same with TRBs of MAIT obtained from TCRdb. Density of the obtained TRBs was 1,851 and mean of frequency was 0.1%. In pCR and non-pCR groups, density, richness, and frequency were consistently higher in pCR group, but it was statistically not significant (**Table 11, Figure 9C).**

Table 12. Immune repertoire of MAIT according to the treatment response

	pCR[1] (n=13)	Non-pCR[2] (n=10)	*p*-value
Classical MAIT[3] (by V, J usage)			
TRA			
Density (mean)	60.3	163.4	0.756
Richness (mean)	22.4	17.1	0.733
Frequency (mean) (%)	0.4	0.09	0.376
TRB			
Density (mean)	9,283.3	7,882.1	0.692
Richness (mean)	1381.2	1082.6	0.313
Frequency (mean) (%)	14.9	12.9	0.313
MAIT (by TCRdb database)			
TRB			
Density (mean)	110.2	41.9	0.456
Richness (mean)	9.5	7.7	0.641
Frequency (mean) (%)	1.7	0.07	0.368

[1]pCR, pathologic complete response; [2]non-pCR, non-pathologic complete response; [3]MAIT, mucosa-assicuated invariant T cells

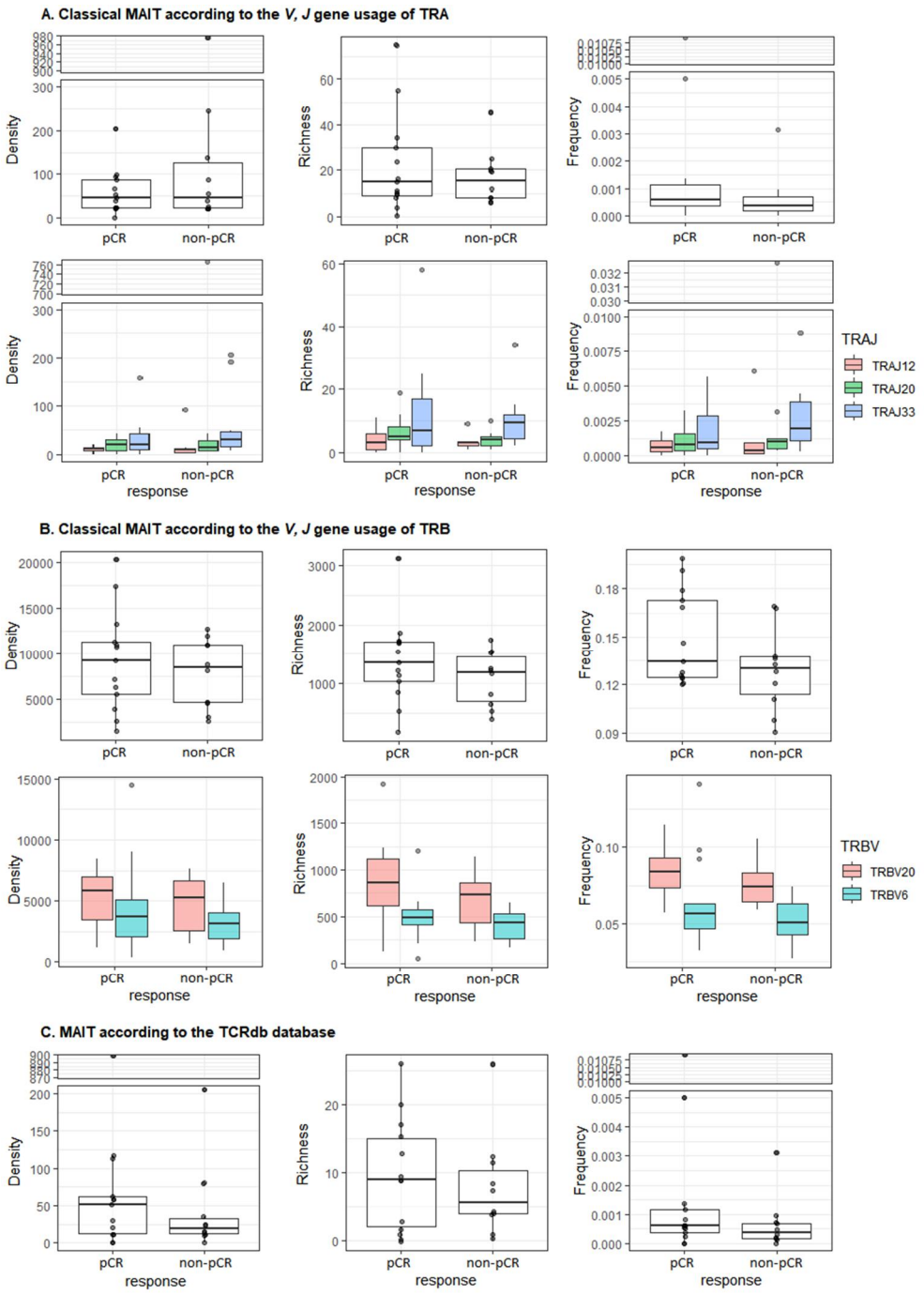

Figure 9. MAIT according to TCHP response. A&B. Density, richness, and frequency of classical MAIT assumed by V and J usage are not significantly different in CR and non-pCR group. C. MAITs assumed by published data of TCRdb also show no significant difference between CR and non-pCR groups.

3.6. Public TCRs and specific TCR sequences

Totally, 1,231,998 TRBs of healthy patients (public TCR) were collected from the vdjdb, of which 18,373 TRBs had the same V, D, and J gene and CDR3 amino acid as the TRB data in current study. When comparing pCR and non-pCR groups, mean of density, richness, and frequency was not significantly different in both groups (**Table 12, Figure 10A**).

Miri Gordin, *et al*. reported public TCR between human and mouse model of mammary tumor in humans and the HER2/neu/ERBB2 human breast cancer mouse model (21). They reported "CASSLSYEQYF" and "CASSLSYEQYF" were dominant CDR3 sequences in cross-species TCRs. In our studies, "CASSLSYEQYF" and "CASSLSUEQYF" sequences were also present, and 1,069 sequences which differ from CASSLGYEQYF and CASSLSYEQYF by 1 or 2 amino acids were founded. However, these CDR3 sequences did not statistically explain the difference between CR and non-pCR groups (**Table 12, Figure 10B**).

TP53 mutation, the most common mutation of human cancer, has been founded up to 72% of HER2 positive breast cancer (22). We also searched mutant *TP53* (R175H, Y220C, G245S, R248W) targeting TCR sequences in TCRdb and TCR3d, and 12 sequences were founded (**Table 9**). Based on these sequences, we extracted similar sequences, and 47 sequences of TRA and 15 sequences of TRB were found. In both TRA and TRB, the density, richness, and frequency of p53 targeting sequences were not significantly different between pCR and non-pCR groups (**Table 12, Figure 10C**).

A HER2 targeting sequence was also searched on TCRdb (**Table 13**), and 1 of TRA and 3 of TRB similar sequences were found. All of the similar sequences were found in pCR group (**Table 12**).

The shared sequences between pre-TCHP and post-TCHP in the preliminary experiment, were searched in the main experiment. Totally, 325 sequences in TRA and 421 sequences in TRB were identified as the similar sequences with the shared sequences of the preliminary experiment. The distribution of these shared sequences were not significantly different between pCR and non-

pCR groups, in the aspect of density, richness, and frequency (**Figure 10D**).

Table 13. Immune repertoires of similar sequences with data from published papers

	pCR[1] (n=13)	Non-pCR[2] (n=10)	*p*-value
Public TCR (TRB, healthy control, vdjdb)			
Density (mean)	7,566.4	8,594.7	0.313
Richness (mean)	840.0	745.3	0.784
Frequency (mean) (%)	17.2	12.3	0.283
CDR3 amino acids "CASSLGYEQYF" & "CASSLSYEQYF"			
Density (mean)	463.5	564.1	0.879
Richness (mean)	52	39.3	0.077
Frequency (mean) (%)	0.8	1.0	0.077
p53 targeting TCR sequence			
TRA			
Density (mean)	5.5	4.6	0.573
Richness (mean)	2.3	1.7	0.681
Frequency (mean) (%)	0.04	0.03	0.513
TRB			
Density (mean)	13.9	2.4	0.622
Richness (mean)	0.8	0.5	0.501
Frequency (mean) (%)	0.015	0.003	0.526
HER2 targeting TCR sequences			
TRA			
Density (sum)	2	0	NA[3]
Richness (sum)	1	0	NA
Frequency (sum) (%)	0.006	0	NA
TRB			
Density (sum)	6	0	NA

Richness (sum)	3	0	NA
Frequency (sum) (%)	0.008	0	NA
Shared TCR sequences of preliminary experiment			
TRA			
Density (mean)	1020.1	1156.8	0.831
Richness (mean)	13.9	14.4	0.526
Frequency (mean) (%)	5.1	6.2	0.313
TRB			
Density (mean)	3249.8	2802.8	0.831
Richness (mean)	18.6	17.9	0.803
Frequency (mean) (%)	4.8	4.4	0.648

[1]pCR, pathologic complete response; [2]non-pCR, non-complete response; [3]NA, not applicable

Table 14. p53 and HER2 targeting TCR sequences from vdjdb and TCR3d

TRAV	CDR3	TRBV/ TRBJ	CDR3
TP53			
R175H			
TRAV12-1	CVVQPGGYQKVTF	*TRBV6-1*	CASSEGLWQVGDEQYF
TRAV6	CALDIYPHDMRF	*TRBV11-2*	CASSLDPGDTGELFF
TRAV38-1	CAFMGYSGAGSYQLTF	*TRBV10-3/TRBJ1-6*	CAISELVTGDSPLHF
TRAV12-3	CAMSGLKEDSSYKLIF		
TRAV24	CALITGGGNKLTF	*TRBV6-3*	CASRLQGWNSPLHF
TRAV13-1	CAASKSAIMVVLQTSSSL	*TRBV27/ TRBJ2-3*	CASSIQQGADTQYF
Y220C			
TRAV12-2	CAWNSGGSNYKLTF	*TRBV6-3*	CASSYSQAWGQPQHF
TRAV3	CAVRVWDYKLSF	*TRBV19*	CASSISAGGDGYTF
R248W			
TRAV1-2	CAVYTGGFKTIF	*TRBV11-2*	CASNLGGGSTDTQYF
TRAV1-2	CAFYYGGSQGNLIF	*TRBV7-8*	CASSFGSGSTDTQYF
TRAV1-2	CAVYPGGSQGNLIF	*TRBV11-2*	CASSLGTGSTDTQYF
G245S			
TRAV8-1	CAVKGDYKLSF	*TRBV11-2*	CASSLVNTEAFF
HER2			
TRAV8-6	CAVSVNTDKLIF	*TRBV20-1/*	CSAPPLAGDETQYF

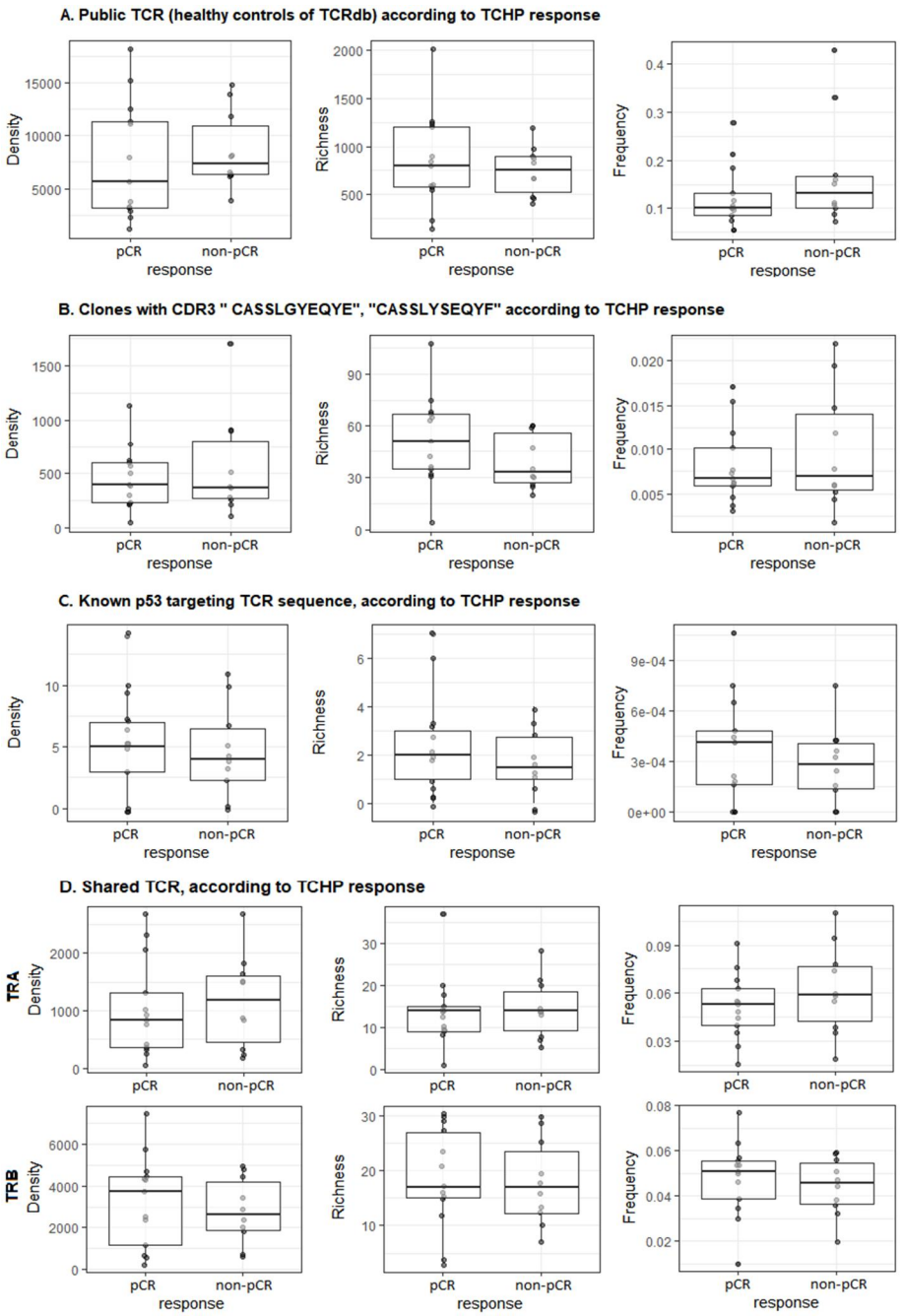

Figure 10. Immune repertoires of similar sequences with data from published papers and preliminary experiment. A. Public TCR of healthy patients. The density, richness, and frequency show no significant difference. B. Previously reported public TCR sequences in HER2/neu breast cancer model (mice) with human. No significant difference is noted in density, richness, and frequency between pCR and non-pCR groups. C. Previously reported p53 targeting sequences. pCR and non-pCR group show similar distribution in density, richness, and frequency. D. Shared TCR between pre- and post-TCHP in preliminary experiment, according to TCHP response. Both TRA and TRB show no significant difference in pCR and non-pCR groups.

3.7. Characteristics of Immune Repertoire according to the TILs

Some studies have been reported that the level of TILs is significantly associated with pCR in HER2 positive breast cancer (6, 23). For the exclusion of effect of TILs, we subdivided the treatment response group according to the level of TILs as high and low TIL. The clinicopathologic characteristics of the four groups, pCR/highTIL, non-pCR/highTIL, pCR/lowTIL, and non-pCR/lowTIL, were summarized in **Table 14**. When comparing pCR/highTIL and non-pCR/highTIL, none of parameters showed significant difference. Most of the comparison of pCR/lowTIL and non-pCR/lowTIL had no significant difference, but lymph node metastasis showed significantly higher frequency in non-pCR/lowTIL ($p < 0.001$), (**Table 14**).

In TCR, there was no difference in mean of SDI, density, and richness of TRA, TRB, TRD, and TRG (**Table 15, Figure 11**). The composition of the clones was significantly different in pCR/highTIL vs. non-pCR/highTIL and pCR/lowTIL vs. non-pCR/lowTIL ($p < 0.001$, respectively). However, only < 0.01% and 0.1~0.01% of TRA and TRB showed a difference of more than 10%, when comparing pCR/lowTIL and non-pCR/lowTIL. In TRA of non-pCR/lowTIL, 0.01~0.1% category was 63.0% and < 0.01% category was 32.9%, while in TRA of non-pCR/lowTIL, 0.01~0.1% category was 45.3% and < 0.01% category was 51.8%. Similar results were shown in TRB of pCR/lowTIL and non-pCR/lowTIL (pCR/lowTIL, 0.01~0.1%, 14.7%; < 0.01%, 84.1% and non-pCR/lowTIL, 0.01~0.1%, 26.5%, and < 0.01%, 72.0%) (**Figure 11**). The proportion of TRGV9 and TRDV2, which represent Vγ9Vδ2 T cells, were not significantly different in pCR and non-pCR groups (**Table 15**).

The CDR3 sequences with a stop codon or out of frame for amino acid was classified as a non-productive TCR. In both TRA and TRB, frequency of non-productive TCR was higher in non-pCR/lowTIL group than pCR/lowTIL group, and it was statistically significant in TRB ($p = 0.002$). In the lowTIL group, when drawing a receiver operating characteristic (ROC) curve predicting treatment response with frequency of non-productive TCR, area under curve (AUC) was 0.833

and 0.976 in TRA and TRB, respectively. No significant difference was found on the other comparisons (**Table 15, Figure 12**).

Table 15. Clinicopathologic characteristics of groups according to TCHP response with TILs

	pCR[1]/ highTIL[2] (n=7)	Non-pCR[3]/ highTIL (n=3)	*p*-value	pCR/ lowTIL (n=6)	Non-pCR/ lowTIL (n=7)	*p*-value
Age (median, range)	47 (38-61)	48 (52-46)	0.748	52 (38-67)	59 (32-71)	0.096
Tumor size (mean ±Std[4])	2.8 ± 1.0	3.5 ± 0.8	0.141	4.7 ± 1.8	4.9 ± 3.2	0.899
TIL (%) (median, range)	10 (10-20)	30 (10-30)	0.452	0 (0)	0 (0)	1
RCB[5] class (%)						
pCR	7 (100)	0 (0)		6 (100)	0 (0)	
1	0 (0)	0 (0)		0 (0)	3 (43)	
2	0 (0)	2 (67)		0 (0)	1 (14)	
3	0 (0)	1 (33)		0 (0)	3(43)	
RCB score (median, range)	0 (0)	1.639 (1.388-4.039)		0 (0)	2.493 (0.790-4.067)	
Histologic grade (%)			0.558			0.899
1	0 (0)	0 (0)		0 (0)	0 (0)	
2	4 (57)	2 (67)		3 (50)	3 (43)	
3	3 (43)	1 (33)		3 (50)	4 (57)	
Lymph node metastasis (%)	0 (0)	1 (33)	0.445	0 (0)	4 (57)	**< 0.001***
Hormonal receptor (%)			0.260			0.391
Negative	5 (71)	1 (33)		4 (67)	3 (43)	
Positive	2 (29)	2 (67)		2 (33)	4 (57)	
HER2 3+	6 (86)	3 (100)	0.490	6 (100)	4 (57)	0.067

[1]pCR, pathologic complete response; [2]TIL, tumor infiltrating lymphocytes; [3]non-pCR, non-pathologic complete response; [4]Std, standard deviation; [5]RCB, residual cancer burden; *$p < 0.05$

Table 16. TCR repertoires of groups according to TCHP response with TILs

	pCR[1]/ highTIL[2] (n=7)	Non-pCR[3]/ highTIL (n=3)	*p*-value	pCR/ lowTIL (n=6)	Non-pCR/ lowTIL (n=7)	*p*-value
SDI[4] (mean)						
TRA	6.845	6.816	0.833	6.751	6.556	0.294
TRB	7.508	7.342	0.383	7.395	7.296	0.538
TRD	3.566	4.404	0.267	3.886	3.478	0.294
TRG	2.479	2.765	0.516	2.545	2.332	0.234
Density (mean)						
TRA	16,082	18,992	0.833	14,661	13,413	0.945
TRB	68,850	78,524	0.667	49,447	47,281	0.835
TRD	351	870	0.067	473	317	0.730
TRG	282	690	0.183	429	320	0.5338
Richness (mean)						
TRA	3,941	4,023	1	4,489	2,967	0.6282
TRB	10,097	9,472	0.833	9,589	7,229	0.6282
TRD	121	224	0.183	184	112	0.294
TRG	100	181	0.267	160	92	0.445
Composition (mean)						
TRA (%)						
1~ 10%	9 (0)	6 (0)	**< 0.001***	19 (1.0)	15 (1.0)	**< 0.001***
0.1~ 1%	793 (2.8)	362 (3.0)		761 (2.8)	844 (4.1)	
0.01~ 0.1%	15,423 (55.9)	6,121 (50.7)		12,202 (45.3)	13,090 (63.0)	
< 0.01%	11,364 (41.2)	5,582 (46.2)		13,952 (51.8)	6,825 (32.9)	
TRB (%)						
1~ 10%	19 (0)	9 (0)	**< 0.001***	25 (0)	22 (0)	**< 0.001***
0.1~ 1%	739 (1.0)	385 (1.3)		706 (1.2)	735 (1.5)	
0.01~ 0.1%	9,710 (13.7)	3,724 (13.1)		8,441 (14.7)	13,396 (26.5)	
< 0.01%	60,216	24,300		48,362	36,456	

	(85.1)	(85.5)		(84.1)	(72.0)	
TRG (%)						
TRGV9	60 (21.3)	243 (35.2)	0.116	89 (20.7)	67 (20.9)	0.616
Others	222 (78.7)	447 (64.8)	0.303	340 (79.3)	253 (79.1)	0.628
TRD (%)						
TRDV2	173 (49.4)	253 (29.1)	0.383	275 (58.1)	149 (47.2)	0.616
Others	177 (50.6)	617 (70.1)	0.067	198 (41.9)	167 (52.8)	0.628
Non-productive TCR[5] (mean)						
TRA						
Density	1,821.9	1,971.0	1	1,477.8	1,548.6	0.628
Richness	645.9	691.7	0.383	696	494	0.534
Frequency (%)	10.2	9.4	0.183	9.5	10.6	0.051
TRB						
Density	4,016.1	4,515.6	1	2,446	3,075.1	0.366
Richness	1,732.8	1,736.3	0.383	1,217.3	1,277	0.534
Frequency (%)	5.7	5.4	0.156	4.7	6.1	**0.002***

[1]pCR, pathologic complete response; [2]TIL, tumor infiltrating lymphocytes; [3]non-pCR, non-pathologic complete response; [4]SDI, Shannon diversity index; [5]TCR, T cell receptor; * *p*-value <0.05

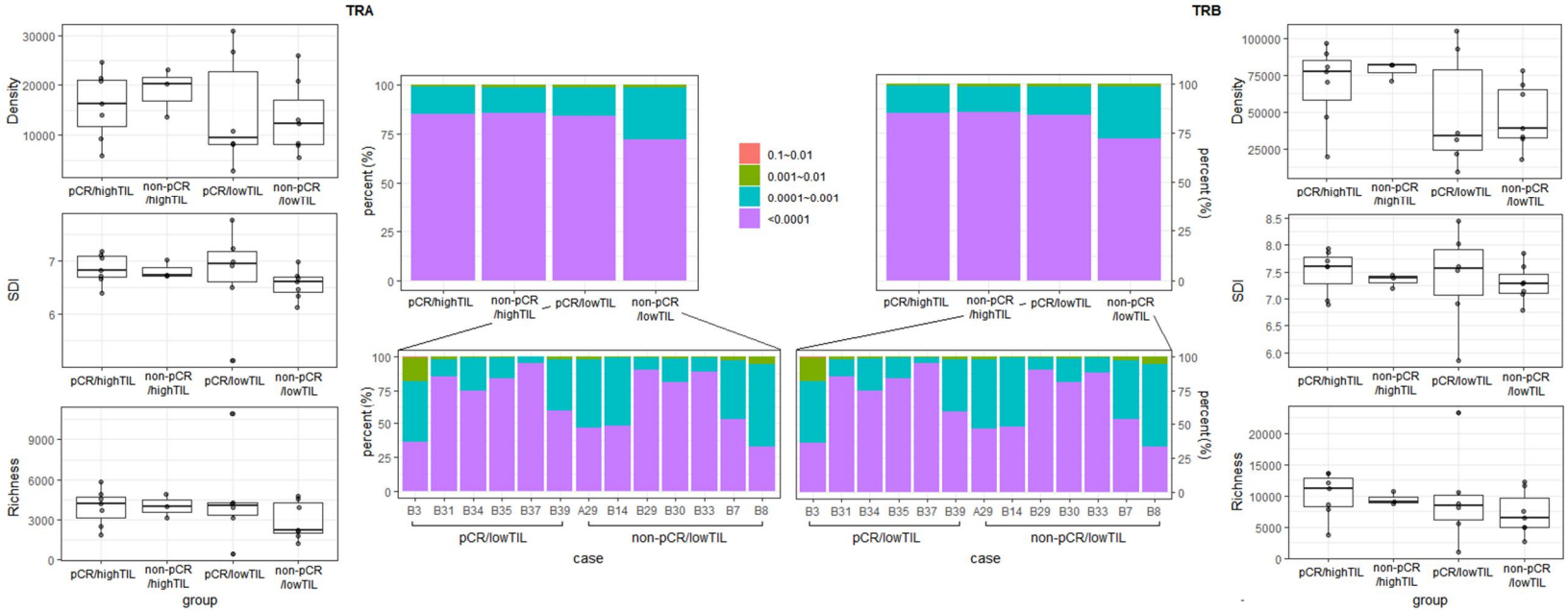

Figure 11. TCR repertoires according to TCHP response with TILs. Density, SDI, richness of TRA and TRB shows no significant difference between pCR/highTIL vs. non-pCR/highTIL, and pCR/lowTIL vs. non-pCR/lowTIL. The composition of low frequency sequences is lower in non-pCR/lowTIL group than pCR/lowTIL group.

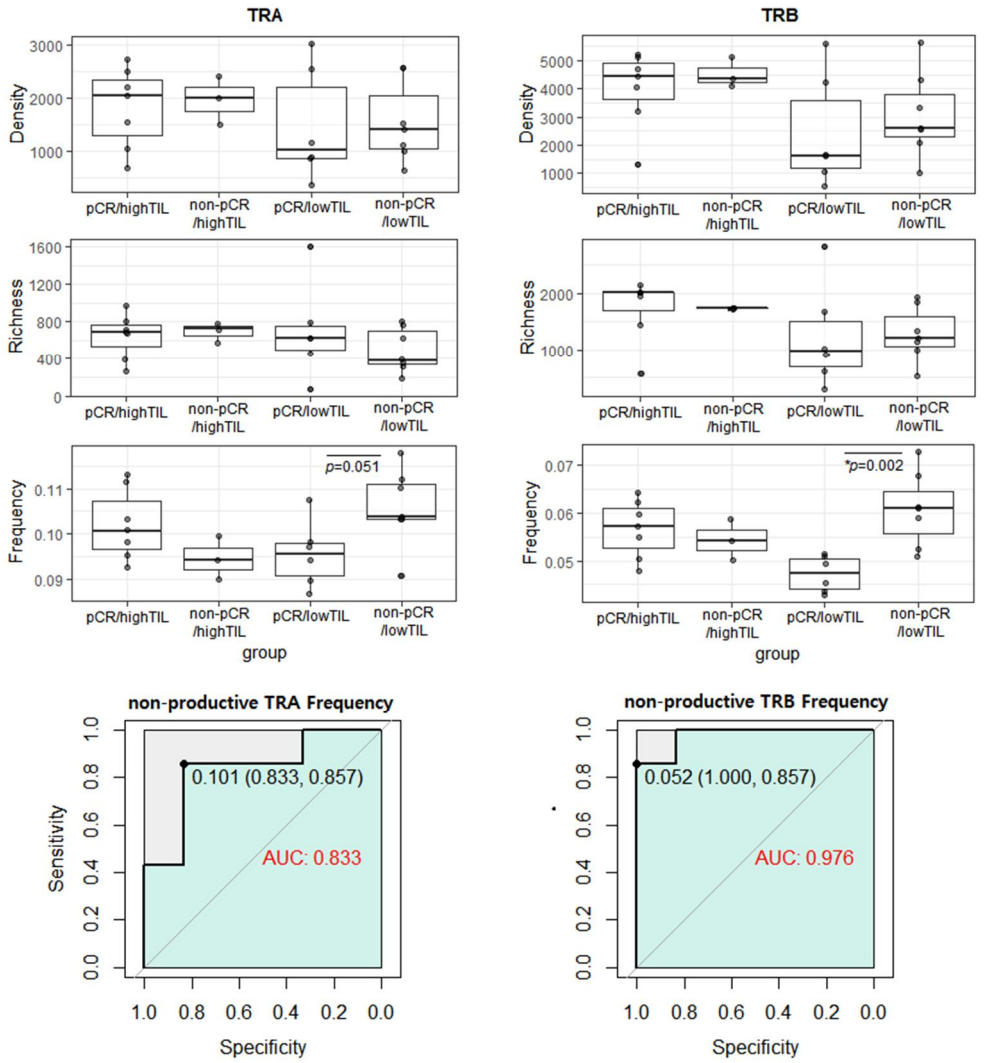

Figure 12. Non-productive TCR according to TCHP response with TILs. The frequency of non-productive TRA and TRB in non-pCR/lowTIL shows significantly higher than pCR/lowTIL. Other comparisons show no difference.
In lowTIL group, frequency of non-productive TCR shows AUC 0.833 in TRA and AUC 0.976 in TRB.

In BCR, all groups showed no significant difference in SDI, density, and richness of IGH, IGK, and IGL. Isotypes of IGH also showed no difference between each group. The composition of IGH, IGL, and IGK showed statistically significant difference ($p < 0.001$), and in the comparison between highTIL groups, non-pCR/highTIL had more < 0.001% category of IGK and IGL (IGK, pCR/highTIL 62.9%, non-pCR/highTIL 72.9%; IGL, pCR/highTIL 31.8%, non-pCR/highTIL 51.0%). In lowTIL groups, IGL showed similar results, non-pCR/lowTIL had more < 0.001% category (pCR/lowTIL 44.0%, and non-pCR/lowTIL 55.4%), and pCR/lowTIL had more 0.001~0.01% category (pCR/lowTIL 32.0%, and non-pCR/lowTIL 55.4%). The other categories showed no difference more than 10%. Hypermutated clones were not significantly different in density, richness, and frequency between pCR/highTIL vs. non-pCR/highTIL and pCR/lowTIL vs. non-pCR/lowTIL (**Table 16, Figure 13**).

Non-productive BCR of density of IGK in non-pCR/highTIL group was significantly higher than pCR/highTIL group. The mean of other parameters of non-productive BCR, richness, density, and frequency of IGH, IGK, and IGL were higher in non-pCR/highTIL group than pCR/highTIL group, but statistically not significant. pCR/lowTIL and non-pCR/lowTIL groups showed no difference (**Table 16, Figure 14**).

None of cases had sequences of IGH, IGK, and IGL similar with trastuzumab and pertuzumab.

Table 17. BCR repertoires of groups according to TCHP response with TILs

	pCR[1]/ highTIL[2] (n=7)	Non-pCR[3]/ highTIL (n=3)	*p*-value	pCR/ lowTIL (n=6)	Non-pCR/ lowTIL (n=7)	*p*-value
SDI[4] (mean)						
IGH	6.161	6.397	1.000	6.219	6.708	0.755
IGK	6.121	5.760	0.667	5.797	7.121	0.573
IGL	5.124	5.513	1.000	5.552	6.371	1.000
Density (mean)						
IGH	707,776	794,986	0.667	709,185	668,712	0.491
IGK	668,675	1,164,079	0.067	780,198	595,456	0.228
IGL	178.790	286,026	0.183	234,046	205,732	0.490
Richness (mean)						
IGH	16,505	28,348	0.667	12,231	15,804	0.950
IGK	10,190	17,810	0.833	7,203	11,675	0.662
IGL	4,486	8,253	0.267	4,026	4,919	0.852
Richness, each isotype (mean)						
IGHM (%)	1,720 (10.4)	2,219 (7.8)	0.953	1,318 (10.7)	1,220 (7.7)	0.176
IGHD (%)	181 (1.1)	162 (0.6)	0.268	176 (1.3)	39 (0.2)	0.581
IGHA (%)	3,418 (20.7)	6,156 (21.7)	0.802	2,922 (23.9)	4,563 (28.9)	0.197
IGHA1	2,199 (64.3)	4,006 (65.1)	0.560	1,896 (64.9)	2,944 (64.5)	0.468
IGHA2	1,216 (35.6)	2,142 (34.8)	0.908	1,024 (35.1)	1,617 (35.5)	0.452
Indeterminate	3 (0.1)	8 (0.1)	0.576	1 (0.0)	2 (0.0)	0.896
IGHG (%)	11,181 (67.8)	19,786 (69.8)	0.915	7,806 (63.8)	9,974 (63.1)	0.075
IGHG1	6,972 (62.3)	12,687 (64.1)	0.385	4,490 (57.5)	6,712 (67.3)	0.840
IGHG2	2,523 (22.6)	4,186 (21.2)	0.352	2,154 (27.6)	2,007 (20.1)	0.582
IGHG3	1,001	1,529	0.087	732	696	0.873

	(9.0)	(7.7)		(9.4)	(7.0)	
IGHG4	255 (2.3)	466 (2.4)	0.223	141 (1.8)	162 (1.6)	0.320
Indeterminate	430 (3.8)	918 (4.6)	0.243	289 (2.7)	397 (4.0)	0.331
Indeterminate	5 (0.0)	25 (0.1)		9 (0.1)	8 (0.1)	0.813
Composition* (mean)						
IGH (%)						
1~ 10%	12 (0.1)	10 (0.0)	<0.001*	10 (0.1)	13 (0.1)	<0.001*
0.1~ 1%	265 (0.7)	56 (0.4)		100 (1.0)	94 (0.6)	
0.01~ 0.1%	914 (4.7)	284 (2.3)		860 (8.2)	2121 (5.8)	
0.001~ 0.01%	3,638 (22.0)	2,029 (16.7)		6,402 (26.2)	5,698 (30.9)	
< 0.001%	11,957 (72.5)	22,827 (80.6)		7,898 (64.5)	9,903 (62.6)	
IGK (%)						
1~ 10%	13 (0.1)	12 (0.1)	<0.001*	11 (0.2)	11 (0.1)	<0.001*
0.1~ 1%	119 (1.2)	100 (0.6)		112 (1.5)	101 (0.9)	
0.01~ 0.1%	899 (8.8)	634 (3.5)		962 (13.4)	1,326 (11.4)	
0.001~ 0.01%	2,753 (27.0)	4,083 (22.9)		2,109 (29.3)	3,925 (33.6)	
< 0.001%	6,405 (62.9)	12,981 (72.9)		4,007 (55.6)	6,311 (54.1)	
IGL (%)						
1~ 10%	14 (0.3)	15 (0.2)	< 0.001*	14 (0.3)	9 (0.2)	<0.001*
0.1~ 1%	222 (2.1)	45 (1.1)		103 (2.6)	88 (2.0)	
0.01~ 0.1%	764 (14.6)	249 (7.0)		853 (21.2)	1,005 (23.4)	
0.001~ 0.01%	2,297 (51.2)	1,439 (40.7)		1,769 (43.9)	2,383 (55.4)	
< 0.001%	1,424 (31.8)	4,207 (51.0)		1,286 (32.0)	818 (19.0)	

Hypermutated IGH (mean)							
	Density	50,414	30,793	0.560	125,174	131,561	0.943
	Richness	2.2	1.3	0.321	2.8	3.4	0.495
	Frequency	0.079	0.042	0.422	0.144	0.172	0.726
Non-productive BCR (mean)							
IGH	Density	4,295.3	5,522	0.383	3,590	3,877	0.755
	Richness	1,692.1	2,520.3	0.383	1,422.2	1,408.3	1.000
	Frequency (%)	0.8	0.7	0.517	0.6	0.8	0.108
IGK	Density	3,068.1	5,745.7	**0.033***	3,166	2,566.9	0.755
	Richness	1,260	1,908	1.000	936	1,141	0.183
	Frequency (%)	0.5	0.5	1.000	0.4	0.6	0.573
IGL	Density	1,367.4	1,855.7	0.383	1,098.5	1,153.8	0.662
	Richness	365.1	618.3	0.184	328.5	729.8	0.755
	Frequency (%)	0.8	0.7	0.517	0.6	0.8	0.108

[1]pCR, pathologic complete response; [2]TIL, tumor infiltrating lymphocytes; [3]non-pCR, non-complete response; [4]SDI, Shannon diversity index. *$p < 0.05$

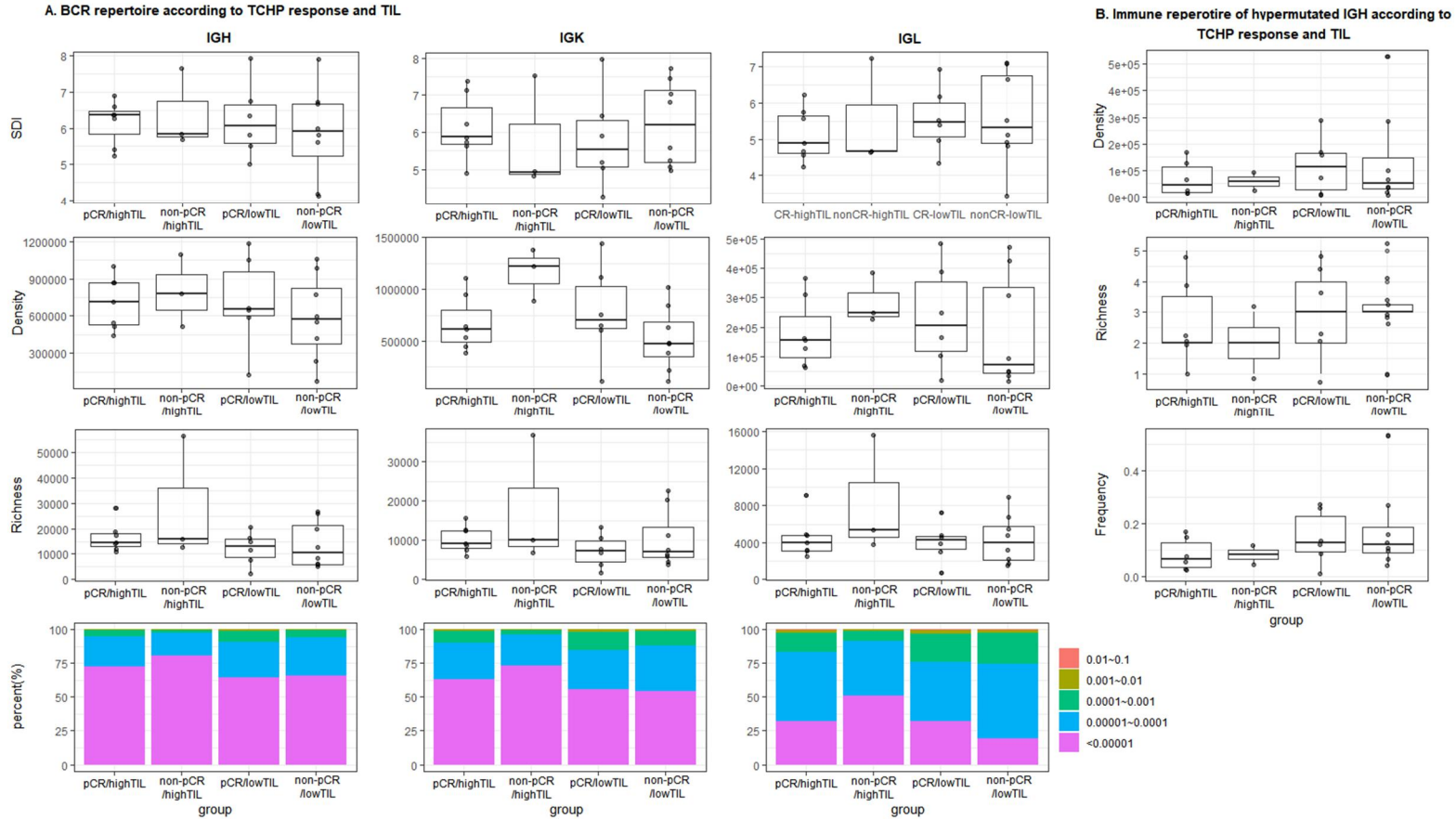

Figure 13. BCR repertoires of groups according to TCHP response with TILs. None of comparison shows significant difference in density, richness, and frequency of IGH, IGL, and IGK. Low frequency clonal composition is consistently higher in non-pCR/highTIL group than pCR/highTIL group in IGH, IGL, and IGK.

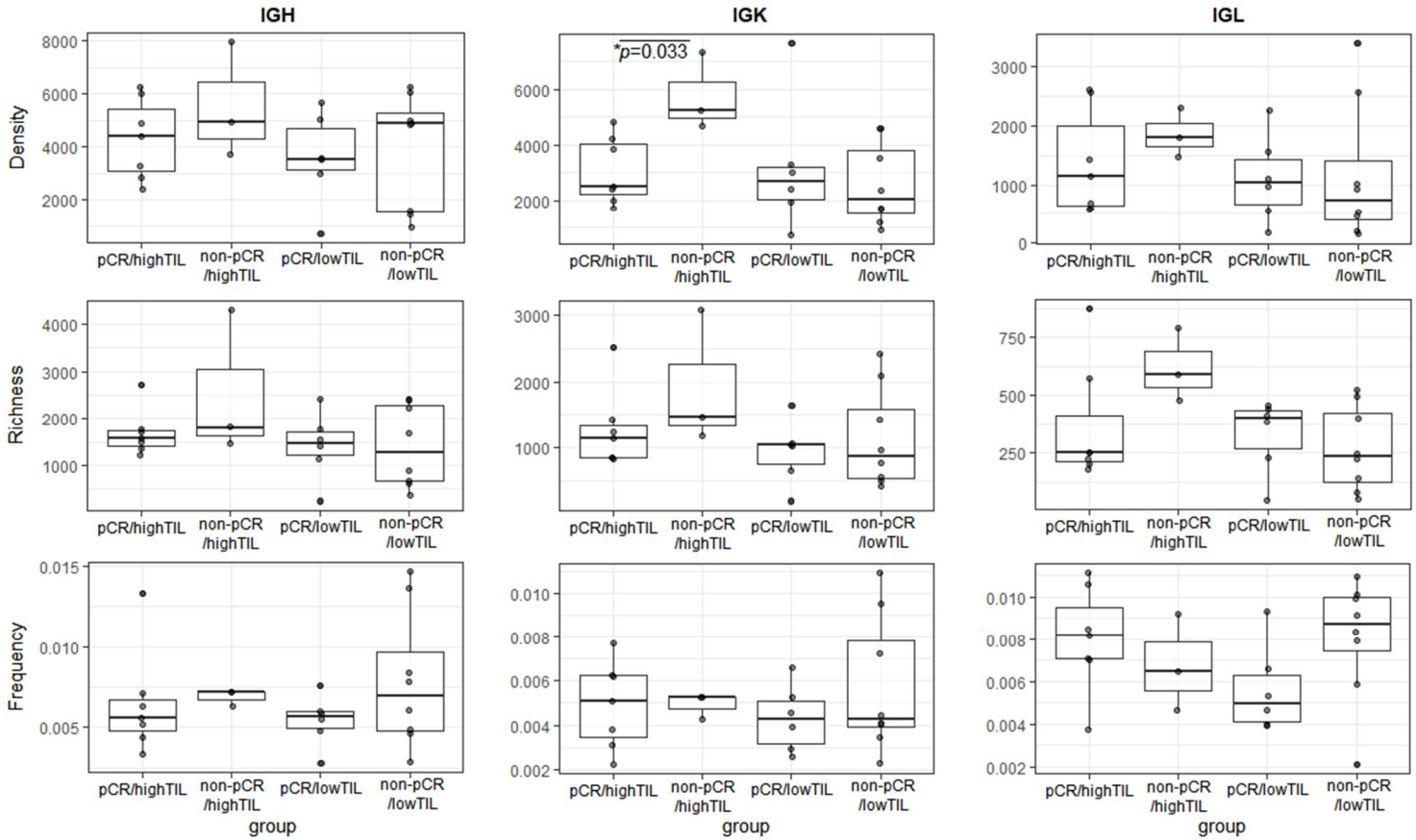

Figure 14. Immune repertoire of non-productive BCR. Density of IGK in non-pCR/highTIL is significantly higher than pCR/highTIL. Mean of density of IGL and richness of IGK and IGL are also higher in non-pCR/highTIL than pCR/highTIL, but statistically not significant.

3.8. Treatment response and gene expression analysis

To understand the characteristics of the tumors with pCR and non-pCR, we analyzed the relationship of the gene expression profile and treatment response. Comparing the gene expression level of non-pCR based on pCR, 185 genes fulfill the condition of differential expression, fold change > 1.5 or < 0.7 and $p < 0.05$, including *ESR1* (estrogen receptor 1) (fold change 6.030, $p = 0.031$, $q = 0.185$) and *PDCD1* (fold change 2.6, $p = 0.049$, $q = 0.104$). However, none of the genes showed significant difference after FDR adjustment. A complete list of these 185 differentially expressed genes was described in **Table 17**, and the heatmap and the volcano plot of these 185 genes expression profile were described in **Figure 15** and **16**, respectively. *HER2 (ERBB2)* and *CD274 (PD-L1)* expression do not meet the criteria of differential expression (*HER2*, fold change 0.565, $p = 0.073$; and *CD274*, fold change 0.815, $p = 0.436$).

To identify the biological processes of differentially expressed genes in each treatment response, DAVID ontological analysis was carried out. The top up-regulated genes in non-pCR included processes of response to steroid hormone (GO: 0048545), regulation of cell shape (GO: 0008360), oxidation-reduction process (GO: 0055114), regulation of ERK1 and ERK2 cascade (GO: 0070372), and negative regulation of cell growth (GO: 0030308) (**Figure 17**).

Based on Prediction Analysis of Microarray 50 (PAM50) classification, HER2-enriched, basal, luminal A, luminal B, normal, and not applicable subtypes were assigned. Nine cases were HER2-enriched (39%), seven cases were luminal A (30%), two cases were luminal B (8%), three cases were normal (13%), and remained two cases were not applicable (8%). HER2-enriched subtypes were more frequently founded on the pCR group (pCR, 7 cases, 54%; non-pCR, 2 cases, 20%), but it was statistically not significant ($p = 0.099$) (**Table 18**, **Figure 18**).

Table 18. List of 185 differentially expressed genes in pCR and non-pCR groups

Gene	Fold change	*p*-value	*q*-value	Gene	Fold Change	*p*-value	*q*-value
ABCA9	0.47	0.044	0.748	*MED12L*	0.26	0.018	0.747
ADAMTS8	0.37	0.029	0.748	*MED13*	0.65	0.026	0.747
ADD2	0.49	0.047	0.748	*MPHOSPH 6*	2.35	0.036	0.748
AFF3	0.21	0.036	0.748	*MTFMT*	0.69	0.042	0.748
AHRR	0.19	0.018	0.747	*MYO15A*	0.47	0.008	0.747
AIFM2	0.59	0.000	0.736	*MYOM1*	0.58	0.044	0.748
ALDH1A2	0.34	0.003	0.747	*NDUFAF6*	0.63	0.049	0.748
AMDHD1	0.63	0.048	0.748	*NEFH*	0.04	0.016	0.747
ANGPT4	0.02	0.001	0.747	*NRL*	0.18	0.016	0.747
ANO1	0.67	0.008	0.747	*NSF*	2.87	0.030	0.748
ANO3	0.37	0.038	0.748	*NTRK2*	0.60	0.036	0.748
ARSG	0.32	0.036	0.748	*NTSR1*	53.43	0.031	0.748
ARTN	0.39	0.038	0.748	*OGN*	0.47	0.018	0.747
ASTN1	0.31	0.032	0.748	*OPRL1*	0.37	0.008	0.747
ATRNL1	0.40	0.038	0.748	*OSMR*	2.76	0.049	0.748
AUNIP	0.58	0.020	0.747	*OTOF*	0.43	0.004	0.747
AVPI1	0.43	0.011	0.747	*PADI3*	7.27	0.027	0.748
BCAS4	0.33	0.030	0.748	*PBX4*	2.12	0.041	0.748
BLMH	0.64	0.026	0.747	*PDK1*	1.95	0.030	0.748
BTN2A2	1.65	0.030	0.748	*PDK2*	0.62	0.012	0.747
C2CD6	0.13	0.001	0.736	*PDSS1*	1.75	0.016	0.747
CACNA1A	0.61	0.018	0.747	*PFN2*	0.50	0.003	0.747
CACNA1G	0.37	0.022	0.747	*PGGHG*	1.84	0.026	0.747
CASQ2	0.39	0.006	0.747	*PIGZ*	0.62	0.049	0.748
CBLN2	0.03	0.048	0.748	*PIR*	0.59	0.012	0.747
CCDC170	0.48	0.012	0.747	*PLPBP*	0.55	0.021	0.747
CCL22	3.20	0.041	0.748	*POLR1F*	2.10	0.028	0.748
CDKN1C	0.29	0.006	0.747	*PPAT*	1.95	0.030	0.748
CFAP20	1.77	0.049	0.748	*PPP1R9B*	0.66	0.026	0.747

CGREF1	0.57	0.010	0.747	*PTN*	0.59	0.018	0.747
CHRNA2	0.08	0.022	0.747	*PTPRR*	0.35	0.048	0.748
CLTRN	9.41	0.031	0.748	*RAB15*	0.67	0.000	0.736
COL2A1	0.07	0.001	0.736	*RCAN3*	2.33	0.042	0.748
COL4A4	2.18	0.010	0.747	*RFX2*	0.61	0.042	0.748
CORO2B	0.53	0.010	0.747	*RGS11*	0.38	0.026	0.747
CPNE3	0.64	0.012	0.747	*RNF185*	1.93	0.035	0.748
CROCCP3	0.50	0.022	0.747	*RPS6KA6*	0.61	0.041	0.748
CTH	0.68	0.032	0.748	*RSAD1*	0.56	0.049	0.748
CYP46A1	0.61	0.021	0.747	*S100A8*	4.51	0.023	0.747
DCDC2	0.62	0.041	0.748	*SCGB2A1*	17.88	0.048	0.748
DDHD2	0.65	0.049	0.748	*SCN1B*	0.58	0.021	0.747
DEPDC1	0.59	0.012	0.747	*SELENOK*	0.68	0.006	0.747
DHDH	0.12	0.022	0.747	*SESN3*	0.62	0.018	0.747
DUSP26	0.08	0.027	0.748	*SGK3*	0.61	0.036	0.748
EDNRB	0.66	0.032	0.748	*SHD*	7.78	0.045	0.748
ELMOD1	0.33	0.031	0.748	*SLC19A2*	0.56	0.021	0.747
EME1	0.54	0.030	0.748	*SLC24A2*	0.65	0.049	0.748
ENKD1	1.95	0.025	0.747	*SLC26A10*	0.58	0.012	0.747
EPN3	0.49	0.042	0.748	*SLC26A3*	0.03	0.022	0.747
FAM117A	0.70	0.012	0.747	*SLC35B1*	0.68	0.042	0.748
FAM135B	0.05	0.023	0.747	*SLC35E4*	0.46	0.004	0.747
FGD3	0.63	0.026	0.747	*SLC6A3*	12.25	0.030	0.748
FKBP5	0.62	0.036	0.748	*SMOX*	0.69	0.021	0.747
FLG	13.90	0.009	0.747	*SMYD1*	0.34	0.045	0.748
FNDC11	0.18	0.007	0.747	*SPAG17*	0.34	0.041	0.748
FNIP2	1.83	0.042	0.748	*SPATA20*	0.42	0.012	0.747
FXYD3	0.67	0.042	0.748	*SREBF1*	0.66	0.049	0.748
GAL3ST2	0.55	0.041	0.748	*STC2*	0.27	0.049	0.748
GLT1D1	5.46	0.038	0.748	*SUPT6H*	0.58	0.015	0.747
GMPR	0.61	0.015	0.747	*SYBU*	0.61	0.012	0.747
GOLGA8UP	0.38	0.015	0.747	*SYT5*	0.14	0.022	0.747
GOSR1	0.64	0.015	0.747	*TCTEX1D1*	0.40	0.020	0.747

GPC4	2.22	0.036	0.748	*TEKT5*	0.28	0.003	0.747
GPRC5A	0.58	0.012	0.747	*TF*	0.44	0.003	0.747
GPSM2	0.56	0.012	0.747	*TIAM1*	2.03	0.042	0.748
GRAMD4	1.87	0.015	0.747	*TLDC2*	0.54	0.043	0.748
GRB14	0.40	0.012	0.747	*TMEM40*	5.03	0.008	0.747
H19	2.02	0.021	0.747	*TNFRSF1A*	1.77	0.049	0.748
HMCN2	0.60	0.035	0.748	*TNFRSF8*	3.57	0.037	0.748
HRC	0.33	0.001	0.736	*TNNT2*	2.74	0.008	0.747
HS3ST1	0.49	0.018	0.747	*TP53AIP1*	0.53	0.021	0.747
HSPB11	0.67	0.014	0.747	*TPD52*	0.68	0.005	0.747
IFI6	0.69	0.042	0.748	*TUBB2B*	0.31	0.005	0.747
IGSF9	2.29	0.026	0.747	*TXNDC16*	0.50	0.003	0.747
IKZF4	2.28	0.026	0.747	*UBASH3B*	1.93	0.042	0.748
IL1RL2	0.17	0.002	0.747	*UGCG*	0.59	0.044	0.748
IL32	1.74	0.042	0.748	*UNC13C*	0.26	0.016	0.747
IL5RA	0.55	0.045	0.748	*UPK3A*	0.39	0.021	0.747
INO80C	2.24	0.030	0.748	*USHBP1*	0.69	0.042	0.748
INTS2	0.49	0.030	0.748	*VOPP1*	1.92	0.003	0.747
IQCN	0.70	0.030	0.748	*VSIG2*	0.61	0.015	0.747
ITGA7	0.61	0.001	0.736	*VTN*	0.12	0.017	0.747
KAT7	0.54	0.021	0.747	*WARS2*	0.70	0.001	0.736
KERA	0.35	0.035	0.748	*WASF3*	0.69	0.006	0.747
KIAA0100	0.64	0.030	0.748	*WDR17*	0.42	0.008	0.747
KYNU	2.68	0.038	0.748	*WDR62*	0.68	0.026	0.747
LRRC29	0.62	0.017	0.747	*WNT10A*	7.12	0.010	0.747
LRRC59	0.55	0.010	0.747	*WNT5A*	2.42	0.018	0.747
LUC7L3	0.53	0.001	0.736	*WWP1*	0.63	0.036	0.748
LY86	0.61	0.049	0.748	*ZC2HC1C*	0.53	0.047	0.748
LYPD3	0.64	0.026	0.747	*ZNF331*	0.64	0.026	0.747
LYPD6B	0.23	0.002	0.747	*ZNF385B*	0.26	0.006	0.747
MCTP2	2.04	0.015	0.747	*ZNF689*	0.29	0.001	0.736

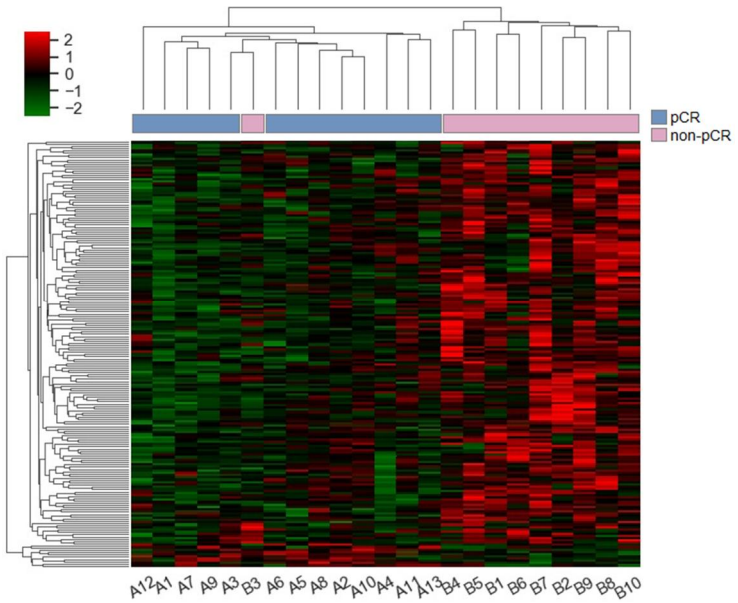

Figure 15. Heatmap of 185 differentially expressed genes between pCR and non-pCR groups. Normalized data is used and scaled to give all genes equal variance. pCR and non-pCR groups are well divided by 185 genes RNA expression.

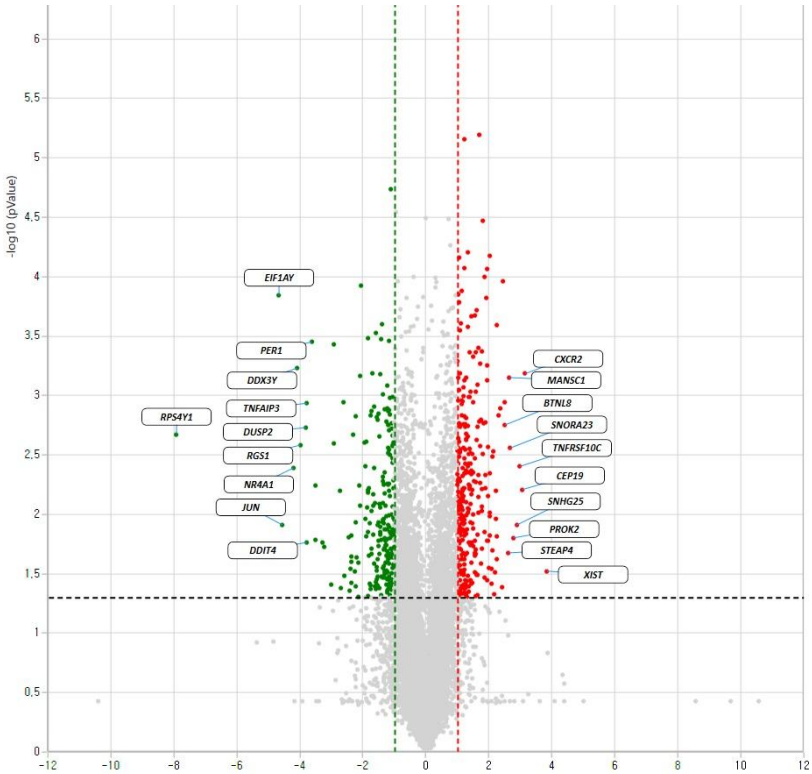

Figure 16. Volcano plot of the differentially expressed genes. The top 10 genes are displayed in the order of fold change.

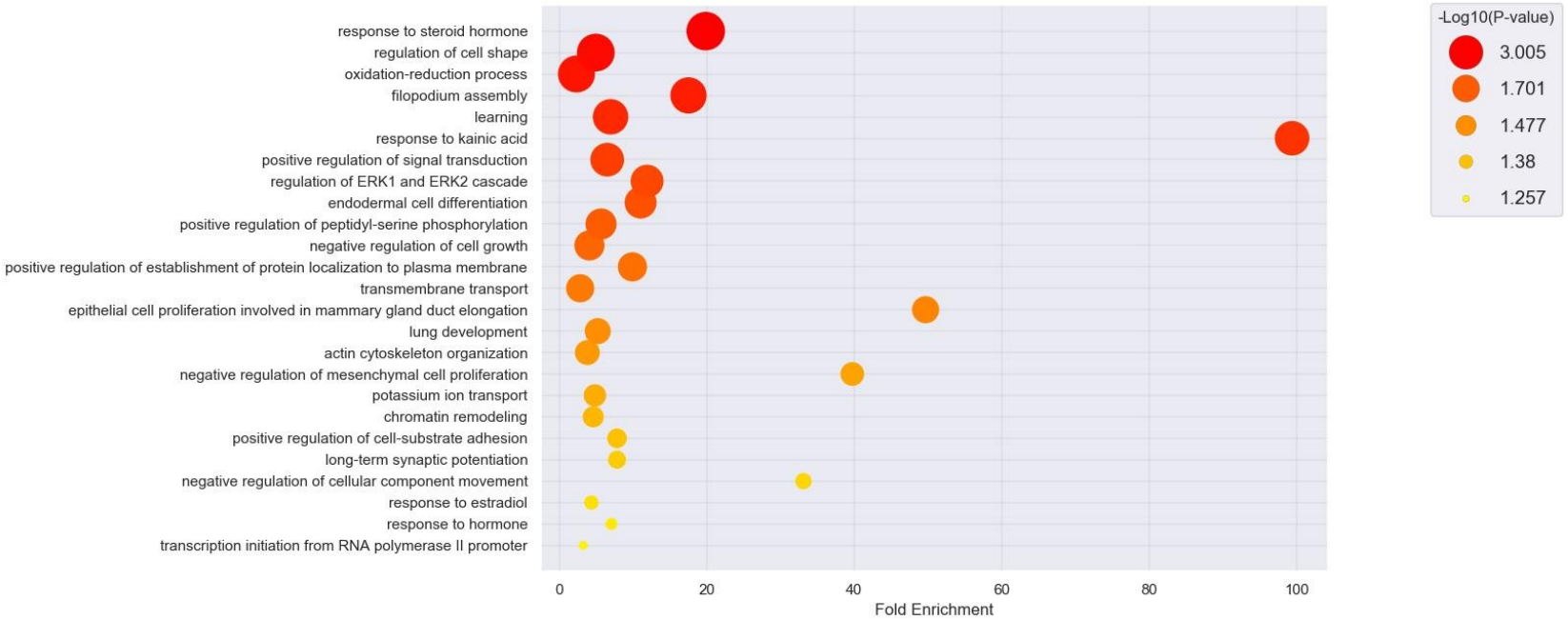

Figure 17. DAVID ontological analysis. Response to kainic acid, response to steroid hormone, filopodium assembly, regulation of cell shape, and regulation of ERK1 and ERK2 cascade were significantly more activated in non-pCR group with fold enrichment >2 and *p*-value < 0.05.

Table 19. PAM 50 classification according to the TCHP response

	pCR[1] (n=13)	Non-pCR[2] (n=10)	*p*-value
PAM[3] 50 classification (%)			0.099
HER2-enriched	7 (54)	2 (20)	
Others	6 (46)	8 (80)	
Luminal A	3 (23)	4 (40)	
Luminal B	1 (7)	1 (10)	
Normal	1 (7)	2 (20)	
Not applicable	1 (7)	1 (10)	

[1]pCR, pathologic complete response; [2]non-pCR, non-complete response; [3]PAM50, prediction analysis of microarray 50;

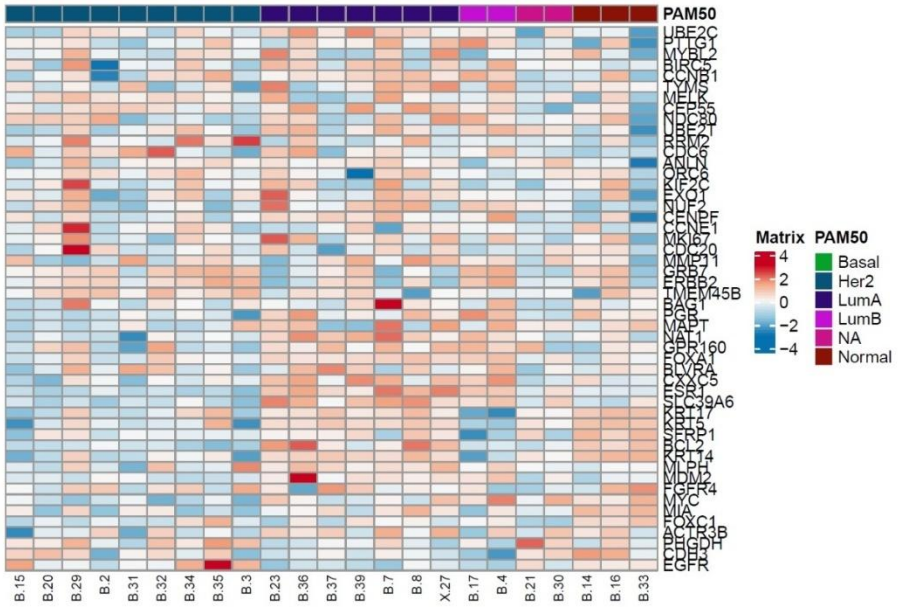

Figure 18. Heatmap of genes of PAM50 classification. Normalized expression data is used.

3.9. Association between Immune repertoire and RNA expression

According to the PAM50 classification, immune repertoire was compared between HER2-enriched subtype and others. Richness, SDI, and density of TCR and BCR showed no significant difference between HER2-enriched subtypes and others (**Table 19**).

When correlation analysis was performed between RNA expression and immune repertoire, 6 genes (*ANKRD7, DPEP3, LGSN, P2RY10, PARP8,* and *SYT6*) were significantly (q-value < 0.05) correlated with richness of TRA, and 2 genes (*PARP8* and *TNGAIP8*) were correlated with TRB. SDI of TRA showed negative correlation with 128 genes. None of the genes showed significant correlation with SDI of TRB. Only *SELPLG* showed high positive correlation with density of TRA (Pearson's coefficient, 0.79, $p < 0.001$, $q = 0.046$), and 5 genes (*BTBD2, NFKBIB, RAC2, TP53,* and *TTC19)* with density of TRB (**Table 20**). On the DAVID ontology analysis, each list of the correlated genes showed no significant gene clustering.

After dividing into pCR and non-pCR, only richness and density of TRB on pCR group showed significant correlation with two genes each (richness, *PARP8*, Pearson's coefficient, 0.86, $q = 0.001$, *TNGAIP8,* Pearson's coefficient, 0.78, $q = 0.037$; density, *POLR1B,* Pearson's coefficient, -0.92, $q = 0.029$; *STK25,* Pearson's coefficient, -0.93, $q = 0.029$). None of other parameters showed significant correlation with RNA expression.

Table 20. Immune repertoire according to the PAM50 classification

Immune repertoire (mean)		HER2 enriched (n=9)	Others (n=14)	*p*-value
TIL[1]		10	10	0.992
TRA	Richness	3,641	3,900	0.758
	SDI[2]	6.654	6.778	0.609
	Density	14,329	15,890	0.649
TRB	Richness	8,854	9,111	0.893
	SDI	7.368	7.409	0.871
	Density	57,980	58,812	0.949
IGH	Richness	12,016	17,531	0.819
	SDI	5.974	6.080	0.193
	Density	526,380	735,132	0.144
IGK	Richness	7,651	11,471	0.172
	SDI	5.974	6.080	0.824
	Density	618,474	714,449	0.547
IGL	Richness	3,768	5,072	0.284
	SDI	5.449	5.303	0.720
	Density	181,068	215,987	0.625

[1]TIL, tumor infiltrating lymphocyte; [2]SDI, Shannon diversity index

Table 21. List of genes associated with immune repertoire

Group	TCR	Immune repertoire	*Gene*	Pearson's coefficient	*p*-value	*q*-value
pCR[1] & non-pCR[2]	TRA	Richness	*ANKRD7*	0.55	< 0.001	0.037
			DPEP3	0.58	< 0.001	0.037
			LGSN	0.50	< 0.001	0.037
			P2RY10	0.52	< 0.001	0.037
			PARP8	0.61	< 0.001	0.008
			SYT6	0.54	< 0.001	0.037
		SDI[3]	*ADM2*	-0.67	< 0.001	0.043
			AFTPH	-0.69	< 0.001	0.033
			ALLC	-0.68	< 0.001	0.036
			ALPK1	-0.71	< 0.001	0.026
			AMBRA1	-0.76	< 0.001	0.025
			APOBEC1	-0.71	< 0.001	0.026
			ARG1	-0.71	< 0.001	0.026
			ASS1	-0.71	< 0.001	0.026
			ATP2B3	-0.71	< 0.001	0.026
			B4GALNT3	-0.71	< 0.001	0.026
			BRINP1	-0.72	< 0.001	0.026
			C6orf118	-0.66	0.001	0.046
			C9orf78	-0.68	< 0.001	0.039
			CAPN15	-0.82	< 0.001	0.010
			CBX8	-0.69	< 0.001	0.033
			CDK13	-0.66	0.001	0.047
			CDK18	-0.69	< 0.001	0.034
			CDK5RAP1	-0.73	< 0.001	0.026
			CDK6	-0.69	< 0.001	0.033
			CDKN2A	-0.70	< 0.001	0.028
			CELA2A	-0.70	< 0.001	0.028
			CHRNA4	-0.69	< 0.001	0.031
			COQ3	-0.67	< 0.001	0.043
			CRHR1	-0.68	< 0.001	0.037

CYP2W1	-0.71	< 0.001	0.026
DDX31	-0.67	0.001	0.045
DDX3Y	-0.71	< 0.001	0.026
DGKD	-0.66	< 0.001	0.045
DGKZ	-0.75	< 0.001	0.026
DLG1	-0.67	0.001	0.045
DUOXA1	-0.71	< 0.001	0.026
EFR3B	-0.71	< 0.001	0.026
EIPR1	-0.67	< 0.001	0.043
EPHA5	-0.70	< 0.001	0.028
ETAA1	-0.68	< 0.001	0.039
F12	-0.72	< 0.001	0.026
FBXL15	-0.78	< 0.001	0.023
GABRA4	-0.71	< 0.001	0.026
GMCL1	-0.71	< 0.001	0.026
GNAO1	-0.69	< 0.001	0.031
GOSR2	-0.72	< 0.001	0.026
GTF3C2	-0.67	0.001	0.045
GTF3C4	-0.71	< 0.001	0.026
HAPLN1	-0.66	0.001	0.047
HAUS2	-0.71	< 0.001	0.026
HCN2	-0.72	< 0.001	0.026
HILPDA	-0.67	< 0.001	0.042
HNRNPM	-0.74	< 0.001	0.026
IL36G	-0.71	< 0.001	0.026
IRAK1BP1	-0.73	< 0.001	0.026
KCNJ1	-0.73	< 0.001	0.026
KCNQ2	-0.71	< 0.001	0.026
KDM5A	-0.75	< 0.001	0.025
KDM8	-0.70	< 0.001	0.028
KIAA0586	-0.66	0.001	0.049
L2HGDH	-0.77	< 0.001	0.023
LCN2	-0.69	< 0.001	0.034
LFNG	-0.69	< 0.001	0.033
LHX9	-0.66	0.001	0.048

LRSAM1	-0.72	< 0.001	0.026
MAP3K10	-0.68	< 0.001	0.037
MAPK6	-0.70	< 0.001	0.028
MDN1	-0.82	< 0.001	0.010
MRPS9	-0.73	< 0.001	0.026
MSANTD2	-0.72	< 0.001	0.026
NCAPD2	-0.71	< 0.001	0.026
NDUFAF7	-0.71	< 0.001	0.026
NDUFB9	-0.71	< 0.001	0.026
NIBAN2	-0.67	< 0.001	0.042
NOL10	-0.73	< 0.001	0.026
NSF	-0.71	< 0.001	0.026
NTMT1	-0.67	< 0.001	0.043
NUBP2	-0.68	< 0.001	0.039
OR13C9	-0.70	< 0.001	0.028
PCDHB2	-0.76	< 0.001	0.025
PCDHB3	-0.74	< 0.001	0.026
PCDHB4	-0.71	< 0.001	0.026
PLPPR1	-0.74	< 0.001	0.026
PNPT1	-0.68	< 0.001	0.035
PPP1R1B	-0.66	0.001	0.048
PRLHR	-0.71	< 0.001	0.026
PROZ	-0.69	< 0.001	0.033
PRPH	-0.67	0.001	0.045
PRR7	-0.79	< 0.001	0.015
RABGAP1	-0.68	< 0.001	0.041
RANBP2	-0.69	< 0.001	0.034
REXO4	-0.77	< 0.001	0.025
RGPD3	-0.66	0.001	0.048
RGPD5	-0.68	< 0.001	0.040
RLIM	-0.67	< 0.001	0.043
RRBP1	-0.68	< 0.001	0.035
SCGB1D2	-0.76	< 0.001	0.025
SET	-0.70	< 0.001	0.028
SHF	-0.75	< 0.001	0.025

	SLC13A5	-0.71	< 0.001	0.026
	SLC17A3	-0.71	< 0.001	0.026
	SLC25A31	-0.71	< 0.001	0.026
	SLC25A37	-0.67	< 0.001	0.043
	SNAP91	-0.71	< 0.001	0.026
	SNAPC1	-0.71	< 0.001	0.026
	SNRPN	-0.72	< 0.001	0.026
	SPATA25	-0.66	0.001	0.049
	STRAP	-0.74	< 0.001	0.026
	SURF2	-0.71	< 0.001	0.026
	SURF6	-0.80	< 0.001	0.015
	SYDE1	-0.69	< 0.001	0.033
	TAGLN3	-0.71	< 0.001	0.026
	TBC1D8B	-0.67	< 0.001	0.043
	TENM1	-0.71	< 0.001	0.026
	TEX15	-0.66	0.001	0.046
	TMEM74B	-0.67	< 0.001	0.042
	TMOD3	-0.74	< 0.001	0.026
	TNNC2	-0.66	0.001	0.046
	TPD52L1	-0.68	< 0.001	0.035
	TRAK2	-0.73	< 0.001	0.026
	TRAP1	-0.66	0.001	0.049
	TRIB3	-0.68	< 0.001	0.041
	TRIM41	-0.66	0.001	0.046
	TTF1	-0.67	< 0.001	0.043
	UBAC1	-0.76	< 0.001	0.025
	UBE3C	-0.71	< 0.001	0.026
	USP34	-0.67	< 0.001	0.042
	USP8	-0.67	< 0.001	0.043
	WHRN	-0.66	0.001	0.047
	WNT6	-0.71	< 0.001	0.026
	WNT8B	-0.69	< 0.001	0.033
	YIPF4	-0.70	< 0.001	0.030
	ZNF837	-0.70	< 0.001	0.028
Density	*SELPLG*	0.79	< 0.001	0.046

	TRB	Richness	*PAPR8*	0.86	< 0.001	0.001
			TNFAIP8	0.78	< 0.001	0.047
		SDI	*None*			
		Density	*BPBD2*	-0.78	< 0.001	0.032
			NFKB1B	-0.75	< 0.001	0.045
			TAC2	-0.76	< 0.001	0.045
			TP53	-0.79	< 0.001	0.032
			TTC19	-0.75	< 0.001	0.045
pCR	TRA	Richness	*None*			
		SDI	*None*			
		Density	*None*			
	TRB	Richness	*PARP8*	0.86	< 0.001	0.001
			TNFAIP8	0.78	< 0.001	0.047
		SDI	*None*			
		Density	*POLR1B*	-0.92	< 0.001	0.029
			STK25	-0.93	< 0.001	0.029
Non-pCR	TRA	Richness	*None*			
	& TRB	SDI	*None*			
		Density	*None*			

3.10. Immune cell sorting with CIBERSORT and treatment response

In order to examine the relationship between the composition of immune cells and the treatment response, decomposition of transcriptome sequencing data for immune cell sorting was performed using CIBERSORT. The most common cells of pCR group were M2 macrophages, naïve B cells, and M2 macrophage, naïve B cells and monocytes in non-pCR group, in that order Eosinophils, neutrophils, naïve CD4 T cells, and γδ T cells were barely present. There was no significant difference between pCR and non-pCR (**Table 21, Figure 19**).

Table 22. Results of CIBERSORT according to the TCHP response

Cell types (relative percentage)	pCR[1] (n=13)	non-pCR[2] (n=10)	*p*-value
Naïve B cells	13.4	14.6	0.879
Memory B cells	0.8	0.9	0.542
Plasma cells	5.5	4.8	0.651
CD8 T cells	2.9	2.6	0.286
CD4 T cells, naïve	0.1	0	0.617
CD4 T cells, memory resting	0.8	1.4	0.279
CD4 T cells, memory activated	1.9	1.1	0.360
Follicular helper T cells	8.1	12.2	0.107
Regulatory T cells	5.0	3.5	0.617
γδ-T cells	0	0.2	NA
NK T cells, resting	5.9	5.9	0.732
NK T cells, activated	0.9	1.6	0.647
Monocytes	11.1	10.5	1
Macrophage, M0	7.1	4.9	0.125
Macrophage, M1	2.1	1.4	0.260
Macrophage, M2	22.4	16.6	0.145
Dendritic cells, resting	3.7	4.1	0.823
Dendritic cells, activated	0.7	0.2	0.83
Mast cells, resting	4.1	9.5	0.582
Mast cells, activated	3.4	4.3	0.821
Eosinophils	0	0	NA[3]
Neutrophils	0.1	0	NA

[2]pCR, pathologic complete response; [2]non-pCR, pathologic non-complete response and [3]NA, not applicable.

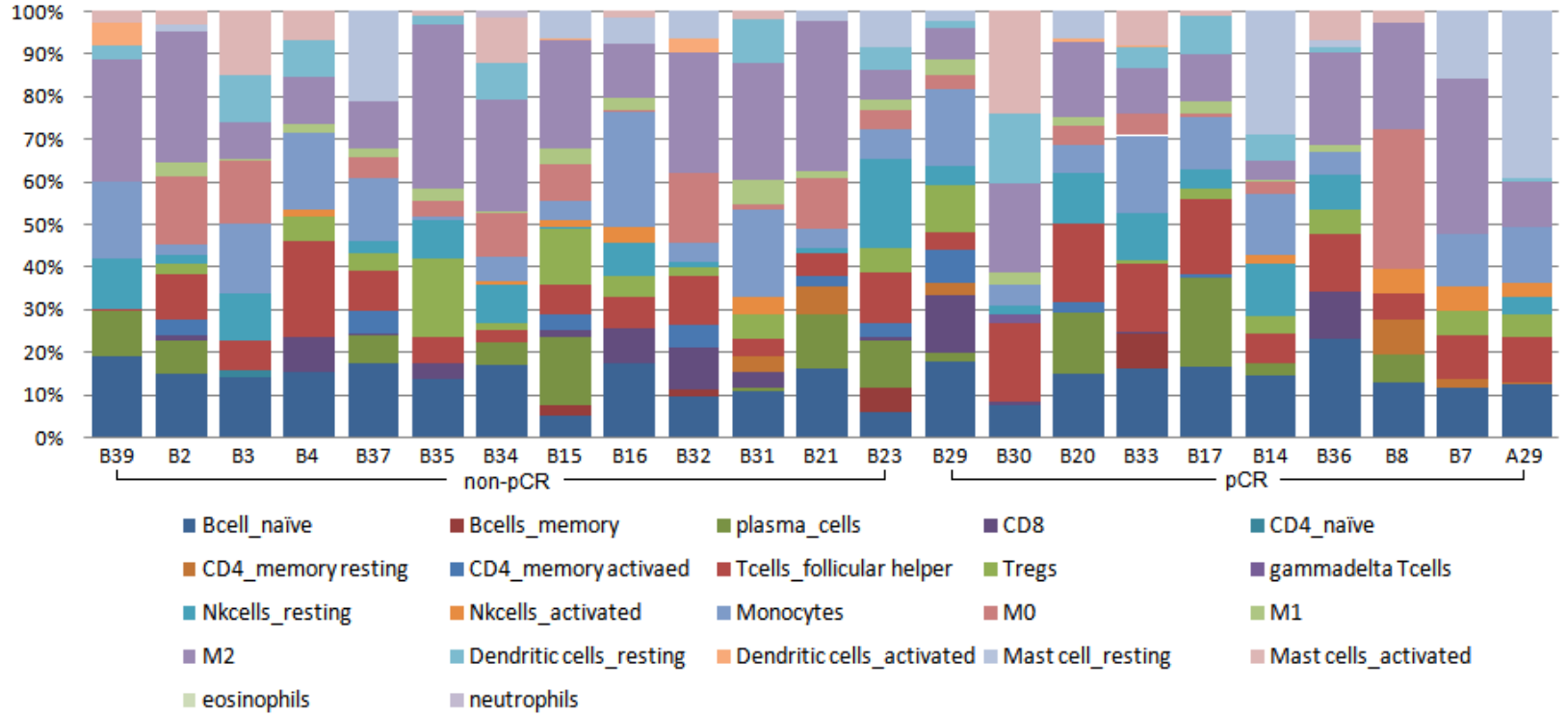

Figure 19. Results of CIBERSORT. None of cell types showed significant difference between the TCHP response groups.

4. DISCUSSION

T cells and B cells are function as an essential components of humoral and cellular immune system, and it has been found that the TCR and BCR repertoire have an important impact on a wide range of disease, including malignancy, autoimmune disorder, and infectious disease (7-9, 24-26). To the best of our knowledge, our study is the first to describe the characteristics of wide range of immune repertoires of T cells (TRA, TRB, TRG, and TRD) and B cells (IGH, IGK, and IGL) in the tumor tissue of HER2 positive early-stage breast cancer and the first to observe changes of immune repertoire after TCHP treatment.

There were several previous studies describing the change of immune repertoire after treatment. Liu *et al.* reported increase in SDI on the TCR of non-small cell lung cancer after several lines of treatment (chemotherapy, radiotherapy, and tyrosine kinase inhibitor therapy) exhibited durable clinical benefit and longer progression free survival (27). On the contrary, another report described the immune depletion and suppressed T cell immunity after the adjuvant chemotherapy (28, 29). In the current study, we observed a decrease in diversity, richness, and density in TCR and density and richness of BCR repertoire after TCHP treatment in preliminary experiment. SDI of BCR was increased after TCHP treatment. This was thought to be associated with immune cell depletion after therapy (28), in that it had nothing to do with the presence or absence of a residual tumor.

The findings of the main experiment showed no significant difference between the pCR and non-pCR groups in the richness, density, and SDI of immune repertoire in both TCR and BCR. In addition, when comparing to the response groups divided into pCR/highTIL, non-pCR/highTIL, pCR/lowTIL, and non-pCR/lowTIL, no difference was identified. Also, in the isotypes of BCR and hypermutated BCR which is the evidence of antigenic stimulation, there was no significant difference between pCR and non-pCR groups. These results are somewhat contrary to previous study of Casarrubios *et al.* which reported about T cell repertoire of non-small cell lung cancer that low evenness of TCR in tumor tissue

and a high percentage of the top 1% sequences showed a significant association with pCR (7). Rui *et al.* also reported the better prognosis in high SDI of cervical cancer patient with concurrent chemotherapy (29). However, although only TRB was examined, the previous report of Force *et al.* of immune repertoires in HER2 positive tumors did not find a significant difference in the immune repertoire of TRB in pre-treatment biopsy, as in the current study (1). This might be due to the tumor's characteristics, which were less likely to be immunogenic because the HER2 positive breast cancer had a lower tumor mutation burden than the non-small cell lung cancer, and had less neo-antigens (30-32).

In BCR repertoire, higher IGHM and lower IGHA was reported in colorectal cancer compared with normal mucosa (26), and in the tumor microenvironment, B cells are dominated by IgM that exhibits high somatic hypermutation rate (33). In the current study, no isotype difference according to the TCHP response was noted.

γδ-T cells are an component of innate immune system and possess multiple favorable anti-tumor characteristics (34). In the breast cancer, two groups reported trastuzumab enhances γδ-T cell dependent antibody dependent cell cytotoxicity toward HER2-overexpressing breast cancer cell lines *in vitro*. Vγ9Vδ2 T-cell is the most abundant γδ-T cells subpopulation, which account for approximately 5% of peripheral blood T cells (34). Vγ9Vδ2 has been reported to recognize various cancers, and exert strong anti-tumor effects, by releasing pro-inflammatory cytokine, granzymes, and perforin and engaging of apoptosis inducing receptors. In our study, immune repertoire of TRD and TRG and distribution of TRGV9 and TRDD2 showed no significant difference between pCR and non-pCR groups.

MAIT cells are semi-variant T cells, representing on about 3% of peripheral T cells, which is divided into classical MAIT and others (17). And classical MAIT, accounting for 95% of MAIT cells, is identified via a Vα1.2-Jα33/12/20 TCR and high CD161 expression (17). Emerging data suggest function of MAIT cells for tumor-progression, however, both pro- and anti-tumor functions have been reported (35, 36). In this study, the distribution of estimated MAIT cells (according to the V and J usage and downloaded TCR sequences) was similar in both pCR and non-pCR

groups. However, this study has a limitation in that when estimating MAIT, it was indirectly evaluated with VJ genes, and the evaluation of CD161 could not be performed.

Some of the TCR sequences were shared among individuals, and TCRs found in more than one individual is called public TCRs (37, 38). Teng *et al.* reported "shared TCR (public TCR)" between viral-nasopharyngeal carcinoma and non-viral nasopharyngeal carcinoma, and revealed commonly used sequences with similar V and J usage according to the viral infection status (39). We also evaluated shared/public TCRs. Public TCRs shared between healthy people downloaded from the database, and the current study showed no significant different distribution of public TCRs between pCR and non-pCR groups. Shared sequences, between pre-TCHP and post-TCHP TCRs of the preliminary experiment were selected and adjusted to the main experiment for evaluating the effect on the treatment response. However, the shared sequences showed no significant difference between pCR and non-pCR groups.

The HER2 targeted sequences were observed in one TRA and three TRBs only in the pCR group. However, since it was only observed in small portion of the pCR group, this alone made it difficult to explain the response to TCHP. The sequences of trastuzumab and pertuzumab, which are thought to be anti-HER2 sequences in BCR, were not observed in both preliminary and main experiment.

In addition, the TCR sequences for p53 that had already been reported (40) showed no significant difference between the pCR and non-pCR groups. In addition, we searched for the sequence of inter-species public TCRs found in HER2/neu/erbb2 cancer model mice and human breast cancer patient (21) in this study. It was found on many cases of pCR and non-pCR groups, but there were difficulties in predicting treatment responses with this. In addition, TCR and BCR that still exist after TCHP were selected in the preliminary experiment to find the association of these sequences with response in the main experiment, but no statistically significant results were obtained.

We searched similar sequences with substitution of 1 or 2 amino acids of

CDR3 using Levenshtein distance, according to the criteria used in TCR3d and other papers (14, 21). However, Levenshtein distance is a mathematical method to calculate similarity of two sentences, and it does not take into account the biological similarities of amino acids. PAM or BLOSUM are much more biological methods for assessing the similarity of amino acids (41). However, due to the lack of research results using these methods, it was difficult to determine objective criteria to evaluate the similarity of TCR.

As TCR rearrangement occurs prior to thymic selection, random insertions and deletions in the CDR3 region would result in approximately one-third in-frame and two-thirds out of frame rearrangements (42). Then, in thymic selection, T cells must have an in-frame heterodimer TCR to survive and leave the thymus (42, 43). However, in previous studies on TCR repertoire, there have been studies showing that non-productive TCR is observed in peripheral tissue and blood samples (16). Some authors used those productive and non-productive TCR genes from mature T cells to define unselected and selected repertoires, assuming that the sequence of the non-productive TCR protein is closely related to a non-selected TCR (44). In the current study, non-productive TCRs were observed with significantly higher frequency in non-pCR/lowTIL group compared to the pCR/low TIL group. These results show the potential as a factor predicting the response to TCHP treatment in lowTIL, and additional validation is needed.

Other previous studies have also reported that there is a difference in treatment response according to RNA expression in HER2 positive breast cancer. In this study, the pathways associated with response to steroid hormone, ERK1/ERK2 cascade regulation, and negative regulation of cell growth were up-regulated in the non-pCR group. These results correspond to the pre-existing results that the pCR rate was lower in the ER+ group, and ERK pathway activation is a part of trastuzumab resistance pathway (45). However, the PAM50 classification, which were reported to be significant in the previous study results to be related to the HER2 treatment response, showed no significant difference in this study.

Recently, anti-PD-L1 antibody and anti-PD-1 antibody have been

introduced to treat in various cancers, including advanced HER2 positive breast cancer (46). In the newest systemic review, advanced breast cancer treated with pembrolizumab (anti-PD-1 antibody) showed promising outcomes in PD-L1 positive/HER2 positive breast cancer (47). We also found higher expression of PD-1 gene (*PDCD1*, fold change 2.6, $p = 0.049$) in non-pCR cases. TCR repertoire is emerging as one of the factors predicting the immunotherapy response in melanoma and non-small cell lung cancer (47-49). In HER2 positive breast cancer, a study to find out the correlation between TCR repertoire and immunotherapy will be helpful.

This study has a limitation in that the observation period was too short to observe the survival and progression due to the characteristics of the breast cancer showing relatively long-term survival, although the tissue freshness was high by using recent cases. Since it was not a single-cell TCR repertoire analysis, there is also a limitation in that it is not possible to know what function of cell of each sequence is. Single cell-based research, which includes cell functions, could be a research method that can overcome these limitations.

In summary, in high throughput sequencing, the role of diversity, richness, and density of TCR and BCR repertoire as predictive markers for TCHP treatment response was not confirmed. However, the inclusion of a large number of low frequency sequences was associated with a good treatment response. Certain previously published sequences or public TCRs did not help to explain the treatment response. High sequences of low frequency and high non-productive TCRs were observed high in the non-pCR group in the lowTIL group. If the function of cells together with TCR and BCR sequences can be known through research using single cells, it will be a study that can overcome the limitations of current research. Additional studies on the correlation between immunotherapy response and immune repertoire in HER2 positive breast cancer are also needed.

Bibliography

1. Force J, Howie LJ, Abbott SE, Bentley R, Marcom PK, Kimmick G, et al. Early Stage HER2-Positive Breast Cancers Not Achieving a pCR From Neoadjuvant Trastuzumab- or Pertuzumab-Based Regimens Have an Immunosuppressive Phenotype. Clin Breast Cancer. 2018;18(5):410-7.
2. Genuino AJ, Chaikledkaew U, The DO, Reungwetwattana T, Thakkinstian A. Adjuvant trastuzumab regimen for HER2-positive early-stage breast cancer: a systematic review and meta-analysis. Expert Rev Clin Pharmacol. 2019;12(8):815-24.
3. Senkus E, Kyriakides S, Ohno S, Penault-Llorca F, Poortmans P, Rutgers E, et al. Primary breast cancer: ESMO Clinical Practice Guidelines for diagnosis, treatment and follow-up. Ann Oncol. 2015;26 Suppl 5:v8-30.
4. Gradishar WJ, Anderson BO, Balassanian R, Blair SL, Burstein HJ, Cyr A, et al. NCCN Guidelines Insights: Breast Cancer, Version 1.2017. J Natl Compr Canc Netw. 2017;15(4):433-51.
5. Salgado R, Denkert C, Demaria S, Sirtaine N, Klauschen F, Pruneri G, et al. The evaluation of tumor-infiltrating lymphocytes (TILs) in breast cancer: recommendations by an International TILs Working Group 2014. Ann Oncol. 2015;26(2):259-71.
6. Ignatiadis M, Van den Eynden G, Roberto S, Fornili M, Bareche Y, Desmedt C, et al. Tumor-Infiltrating Lymphocytes in Patients Receiving Trastuzumab/Pertuzumab-Based Chemotherapy: A TRYPHAENA Substudy. J Natl Cancer Inst. 2019;111(1):69-77.
7. Casarrubios M, Cruz-Bermúdez A, Nadal E, Insa A, García Campelo MDR, Lázaro M, et al. Pretreatment Tissue TCR Repertoire Evenness Is Associated with Complete Pathologic Response in Patients with NSCLC Receiving Neoadjuvant Chemoimmunotherapy. Clin Cancer Res. 2021;27(21):5878-90.
8. Liu X, Zhang W, Zhao M, Fu L, Liu L, Wu J, et al. T cell receptor β repertoires as novel diagnostic markers for systemic lupus erythematosus and rheumatoid arthritis. Ann Rheum Dis. 2019;78(8):1070-8.
9. Cui JH, Lin KR, Yuan SH, Jin YB, Chen XP, Su XK, et al. TCR Repertoire as a Novel Indicator for Immune Monitoring and Prognosis Assessment of Patients With Cervical Cancer. Front Immunol. 2018;9:2729.

10. Farshid G, Bilous M, Morey A, Fox S, Lakhani S, Loi S, et al. ASCO/CAP 2018 breast cancer HER2 testing guidelines: summary of pertinent recommendations for practice in Australia. Pathology. 2019;51(4):345-8.
11. Symmans WF, Peintinger F, Hatzis C, Rajan R, Kuerer H, Valero V, et al. Measurement of residual breast cancer burden to predict survival after neoadjuvant chemotherapy. J Clin Oncol. 2007;25(28):4414-22.
12. Ogston KN, Miller ID, Payne S, Hutcheon AW, Sarkar TK, Smith I, et al. A new histological grading system to assess response of breast cancers to primary chemotherapy: prognostic significance and survival. Breast. 2003;12(5):320-7.
13. Chen SY, Yue T, Lei Q, Guo AY. TCRdb: a comprehensive database for T-cell receptor sequences with powerful search function. Nucleic Acids Res. 2021;49(D1):D468-d74.
14. Gowthaman R, Pierce BG. TCR3d: The T cell receptor structural repertoire database. Bioinformatics. 2019;35(24):5323-5.
15. Shugay M, Bagaev DV, Zvyagin IV, Vroomans RM, Crawford JC, Dolton G, et al. VDJdb: a curated database of T-cell receptor sequences with known antigen specificity. Nucleic Acids Res. 2018;46(D1):D419-d27.
16. Cao W, Goronzy JJ. Structural constraints in T-cell repertoire selection predicted by machine learning. Genes Immun. 2021;22(4):203-4.
17. Souter MNT, Eckle SBG. Biased MAIT TCR Usage Poised for Limited Antigen Diversity? Front Immunol. 2020;11:1845.
18. Dash P, Fiore-Gartland AJ, Hertz T, Wang GC, Sharma S, Souquette A, et al. Quantifiable predictive features define epitope-specific T cell receptor repertoires. Nature. 2017;547(7661):89-93.
19. Chen B, Khodadoust MS, Liu CL, Newman AM, Alizadeh AA. Profiling Tumor Infiltrating Immune Cells with CIBERSORT. Methods Mol Biol. 2018;1711:243-59.
20. Parker JS, Mullins M, Cheang MC, Leung S, Voduc D, Vickery T, et al. Supervised risk predictor of breast cancer based on intrinsic subtypes. J Clin Oncol. 2009;27(8):1160-7.
21. Gordin M, Philip H, Zilberberg A, Gidoni M, Margalit R, Clouser C, et al. Breast cancer is marked by specific, Public T-cell receptor CDR3 regions shared by mice and humans. PLoS Comput Biol. 2021;17(1):e1008486.
22. Li K, Liao N, Chen B, Zhang G, Wang Y, Guo L, et al. Genetic mutation profile of Chinese HER2-positive breast cancers and genetic predictors of

responses to Neoadjuvant anti-HER2 therapy. Breast Cancer Res Treat. 2020;183(2):321-32.

23. Luen SJ, Salgado R, Fox S, Savas P, Eng-Wong J, Clark E, et al. Tumour-infiltrating lymphocytes in advanced HER2-positive breast cancer treated with pertuzumab or placebo in addition to trastuzumab and docetaxel: a retrospective analysis of the CLEOPATRA study. Lancet Oncol. 2017;18(1):52-62.

24. Li N, Yuan J, Tian W, Meng L, Liu Y. T-cell receptor repertoire analysis for the diagnosis and treatment of solid tumor: A methodology and clinical applications. Cancer Commun (Lond). 2020;40(10):473-83.

25. Niu X, Li S, Li P, Pan W, Wang Q, Feng Y, et al. Longitudinal Analysis of T and B Cell Receptor Repertoire Transcripts Reveal Dynamic Immune Response in COVID-19 Patients. Front Immunol. 2020;11:582010.

26. Zhang W, Feng Q, Wang C, Zeng X, Du Y, Lin L, et al. Characterization of the B Cell Receptor Repertoire in the Intestinal Mucosa and of Tumor-Infiltrating Lymphocytes in Colorectal Adenoma and Carcinoma. J Immunol. 2017;198(9):3719-28.

27. Liu YY, Yang QF, Yang JS, Cao RB, Liang JY, Liu YT, et al. Characteristics and prognostic significance of profiling the peripheral blood T-cell receptor repertoire in patients with advanced lung cancer. Int J Cancer. 2019;145(5):1423-31.

28. Gustafson CE, Jadhav R, Cao W, Qi Q, Pegram M, Tian L, et al. Immune cell repertoires in breast cancer patients after adjuvant chemotherapy. JCI Insight. 2020;5(4).

29. Li R, Liu Y, Yin R, Yin L, Li K, Sun C, et al. The Dynamic Alternation of Local and Systemic Tumor Immune Microenvironment During Concurrent Chemoradiotherapy of Cervical Cancer: A Prospective Clinical Trial. Int J Radiat Oncol Biol Phys. 2021;110(5):1432-41.

30. Wen Y, Ouyang D, Chen Q, Zeng L, Luo N, He H, et al. Prognostic value of tumor mutation burden and the relationship between tumor mutation burden and immune infiltration in HER2+ breast cancer: a gene expression-based study. Gland Surg. 2022;11(1):100-14.

31. Castle JC, Uduman M, Pabla S, Stein RB, Buell JS. Mutation-Derived Neoantigens for Cancer Immunotherapy. Front Immunol. 2019;10:1856.

32. Reuben A, Zhang J, Chiou SH, Gittelman RM, Li J, Lee WC, et al. Comprehensive T cell repertoire characterization of non-small cell lung cancer.

Nat Commun. 2020;11(1):603.
33. Aizik L, Dror Y, Taussig D, Barzel A, Carmi Y, Wine Y. Antibody Repertoire Analysis of Tumor-Infiltrating B Cells Reveals Distinct Signatures and Distributions Across Tissues. Front Immunol. 2021;12:705381.
34. Hoeres T, Smetak M, Pretscher D, Wilhelm M. Improving the Efficiency of Vγ9Vδ2 T-Cell Immunotherapy in Cancer. Front Immunol. 2018;9:800.
35. Haeryfar SMM, Shaler CR, Rudak PT. Mucosa-associated invariant T cells in malignancies: a faithful friend or formidable foe? Cancer Immunol Immunother. 2018;67(12):1885-96.
36. Yan J, Allen S, McDonald E, Das I, Mak JYW, Liu L, et al. MAIT Cells Promote Tumor Initiation, Growth, and Metastases via Tumor MR1. Cancer Discov. 2020;10(1):124-41.
37. Wang T, Wang C, Wu J, He C, Zhang W, Liu J, et al. The Different T-cell Receptor Repertoires in Breast Cancer Tumors, Draining Lymph Nodes, and Adjacent Tissues. Cancer Immunol Res. 2017;5(2):148-56.
38. Venturi V, Price DA, Douek DC, Davenport MP. The molecular basis for public T-cell responses? Nat Rev Immunol. 2008;8(3):231-8.
39. Teng YHF, Quah HS, Suteja L, Dias JML, Mupo A, Bashford-Rogers RJM, et al. Analysis of T cell receptor clonotypes in tumor microenvironment identifies shared cancer-type-specific signatures. Cancer Immunol Immunother. 2022;71(4):989-98.
40. Wu D, Gallagher DT, Gowthaman R, Pierce BG, Mariuzza RA. Structural basis for oligoclonal T cell recognition of a shared p53 cancer neoantigen. Nat Commun. 2020;11(1):2908.
41. Mount DW. Comparison of the PAM and BLOSUM Amino Acid Substitution Matrices. CSH Protoc. 2008;2008:pdb.ip59.
42. Kondo K, Ohigashi I, Takahama Y. Thymus machinery for T-cell selection. Int Immunol. 2019;31(3):119-25.
43. Sherwood AM, Desmarais C, Livingston RJ, Andriesen J, Haussler M, Carlson CS, et al. Deep sequencing of the human TCRγ and TCRβ repertoires suggests that TCRβ rearranges after αβ and γδ T cell commitment. Sci Transl Med. 2011;3(90):90ra61.
44. Cao W, Goronzy JJ. Structural constraints in T-cell repertoire selection predicted by machine learning. Genes & Immunity. 2021;22(4):203-4.
45. Zazo S, González-Alonso P, Martín-Aparicio E, Chamizo C, Luque M, Sanz-

Álvarez M, et al. Autocrine CCL5 Effect Mediates Trastuzumab Resistance by ERK Pathway Activation in HER2-Positive Breast Cancer. Mol Cancer Ther. 2020;19(8):1696-707.

46. Kyriazoglou A, Kaparelou M, Goumas G, Liontos M, Zakopoulou R, Zografos E, et al. Immunotherapy in HER2-Positive Breast Cancer: A Systematic Review. Breast Care (Basel). 2022;17(1):63-70.

47. Valpione S, Mundra PA, Galvani E, Campana LG, Lorigan P, De Rosa F, et al. The T cell receptor repertoire of tumor infiltrating T cells is predictive and prognostic for cancer survival. Nat Commun. 2021;12(1):4098.

48. Dong N, Moreno-Manuel A, Calabuig-Fariñas S, Gallach S, Zhang F, Blasco A, et al. Characterization of Circulating T Cell Receptor Repertoire Provides Information about Clinical Outcome after PD-1 Blockade in Advanced Non-Small Cell Lung Cancer Patients. Cancers (Basel). 2021;13(12).

49. Kidman J, Principe N, Watson M, Lassmann T, Holt RA, Nowak AK, et al. Characteristics of TCR Repertoire Associated With Successful Immune Checkpoint Therapy Responses. Front Immunol. 2020;11:587014.

Abstract in Korean

Background: Trastuzumab의 도입으로 HER2 양성 유방암의 치료가 크게 발전했음에도 불구하고, HER2 양성 초기 유방암의 약 30-40%가 여전히 병리학적 완전 반응(pCR)에 도달하지 않는다. 면역 레퍼토리는 악성을 비롯한 광범위한 질병에 상당한 영향을 미치는 것으로 보고되고 있다. 우리는 HER2 양성 초기 유방암의 치료 반응을 예측하는 요인을 찾기 위해 T 세포 수용체(TCR) 및 B 세포 수용체(BCR) 레퍼토리를 조사했다.

Material and methods: 수술 전 TCHP로 치료한 HER2 양성 유방암 총 35예를 모집하였다. 전체 사례를 예비 실험 10건과 본 실험 25건으로 총 2개의 실험으로 나누었다. 예비 실험에서는 TCHP 처리 전의 생검 조직과 TCHP 처리 후의 수술 조직을 비교하였다. 본 실험에서는 TCHP 처리 전 생검 조직을 TCHP 처리 반응에 따라 비교하였다. TRA, TRB, TRG 및 TRD에 대한 T 세포 레퍼토리와 IGH, IGK 및 IGL에 대한 B 세포 레퍼토리를 평가했다. Whole transcriptome sequencing도 수행하였다.

Results: 예비 실험에서는 TCHP 반응에 관계없이 TCHP 처리 후 TCR과 BCR의 밀도와 풍부도가 감소하였다. SDI는 TCR에서는 감소하고 BCR에서는 증가하는 경향을 보였다. 본 실험에서 TCR과 BCR 레퍼토리의 CDR3의 SDI, 밀도, 길이는 pCR군과 non-pCR군 간에 유의한 차이를 보이지 않았다. 밀도, 풍부함, MAIT의 빈도, 건강한 사람의 공통 TCR 및 변이 p53을 표적 서열도 유의한 차이를 보이지 않았다. HER2 표적 TCR 서열은 소수의 pCR 그룹에서만 존재했다. pCR 그룹과 non-pCR 그룹을 TIL 수준에 따라 세분화했을 때 밀도, 풍부도 및 SDI는 pCR/highTIL vs. non-pCR/highTIL 및 pCR/lowTIL vs. non-pCR에서 유의한 차이를 보이지 않았습니다. non-pCR/lowTIL군에서 TRA에서 저주파 클론의 비율이 더 높았다 (non-pCR/lowTIL, 0.01~0.1%, 63%,

<0.01%, 32.9% vs. pCR/lowTIL, 0.01~0.1%, 45.3%, <0.01%, 51.8%, p < 0.001) 및 TRB (non-pCR/lowTIL, 0.01~0.1%, 26.5%, <0.01%, 72.0% vs. pCR/lowTIL, 0.01~0.1%, 14.7%, 0.01%, 84.1%, p < 0.001). 비생산적인 TRA 및 TRB의 빈도는 CDR3 서열에 stop codon이 있거나 out of frame이 있는 것으로 pCR/lowTIL군보다 non-pCR/lowTIL군에서 유의하게 높았다 (TRA, non-pCR/lowTIL 10.6%; pCR/lowTIL 9.5%, p = 0.051; TRB, non-pCR/lowTIL 6.1% and pCR/lowTIL 4.7%, p = 0.002). lowTIL군에서 비생산적 TCR의 빈도로 치료 반응을 예측할 때 AUC는 TRA와 TRB에서 각각 0.833과 0.976이었다. 스테로이드 호르몬에 대한 반응, ERK1/ERK2 cascade 조절 및 세포 성장의 음성 조절과 관련된 경로는 non-pCR 그룹에서 높게 발현되었다.

Conclusion: TCHP 치료 반응에 대한 예측 인자로서 TCR 및 BCR 레퍼토리의 다양성, 풍부함 및 밀도의 역할은 확인되지 않았다. 낮은 빈도의 클론이 많은 것과 비생산적 TCR의 빈도가 높은 것은 TCHP 치료 반응의 예측 인자의 후보가 될 수 있지만, 추가적인 검증과 비생산적 TCR의 생리학적 기전에 대한 연구가 필요하다.